MULTIAXIAL CREEP TESTING
OF ROCK AND CONCRETE

by

© KWOK-HUNG LEUNG, B.Eng.

A Thesis
Submitted to the School of Graduate Studies
in Partial Fulfilment of the Requirements
for the Degree
Master of Engineering

McMaster University

November 1980

MASTER OF ENGINEERING (1980)
(Civil Engineering)

McMASTER UNIVERSITY
Hamilton, Ontario

TITLE: MULTIAXIAL CREEP TESTING OF ROCK AND CONCRETE

AUTHOR: Kwok-Hung LEUNG, B.Eng.(Civil Engineering)
(Nova Scotia Technical College)

SUPERVISOR: Dr. John J. Emery

NUMBER OF PAGES: ix, 104

ABSTRACT

The finite element method of simulating tunnel excavations in squeezing ground requires experimental data on multiaxial creep relationships and related characteristics of rock and concrete as input. A servo-controlled test frame, for applying multiaxial stress states to cubical specimens through three independent actuators, was developed. This test system allows the simulation of typical stress levels and stress paths involved during rock excavation, with continous monitoring of loads and displacements through a data acquisition system. The overall equipment development required considerable design and assembly effort. A testing programme for concrete specimens was completed to evaluate the equipment. Finally, conclusions and recommendations were made which provide the necessary information and guidance for future testing to develop multiaxial creep relationships for rocks known to have significant time-dependent behaviour.

ACKNOWLEDGEMENTS

I would like to take this opportunity to express my thanks to the following individuals:

- My supervisor, Dr. John Emery for his patience and guidance throughout this research.
- Mr. Ralph Winterle, Technican, for his assistance in the testing equipment electronics.
- Mr. Bill Sherriff, Technican, for his excellent machining and advice on the construction of the multiaxial testing frame.

To my parents and wife.

TABLE OF CONTENTS

LIST OF TABLES

LIST OF FIGURES

CHAPTER 1

INTRODUCTION

1-1 INTRODUCTION

The two major parameters to be determined for geotechnical materials such as soil, rock and ice are their strength and deformation behaviour. In many cases, the stresses in loaded soil and rock masses are far below ultimate strengths, however, the resulting deformations may still be sufficiently large for failure in terms of serviceability. A notable example of this is the creep movements associated with excavations in squeezing ground which have been the subject of a continuing research programme at McMaster University (Emery, et al, 1978). This thesis considers an experimental aspect of the programme to develop testing equipment for the determination of multiaxial creep relationships.

1-2 BACKGROUND

Solution methods (analytical and numerical) and experimental work in geotechnical engineering are closely related in that they need positive feedback from one another. As a whole, geotechnology advances as each component is improved within this interaction. While the early development of geotechnical engineering (soil mechanics) was based on empiricism, a more logical basis developed starting in the

1920 to 1940 period largely influenced by Terzaghi, that has reached the present state of a careful blend of experience with largely computerized design methods. However, because of the complexity and great variation in the behaviour of earth materials, the necessary characterization data has often logged the ability of approaches such as the finite element method to provide solutions in geotechnical engineering (Zienkiewicz, 1977). For example, little is known about the time-dependency of joint movements in rock during excavation unloading. The development of multiaxial creep relationships discussed herein was based on such a need for rock and construction materials (concrete) input data to existing finite element method programmes for excavation simulation developed by Hanafy and Emery (Emery et al, 1978).

1-3 PURPOSE AND SCOPE

In order to make full use of the finite element method in geotechnical engineering, it is clear that continuing experimental work is critical to develop constitutive relationships and related characterization data. This study focussed on the development of multiaxial creep relationships. A servo-controlled test frame for applying multiaxial stress states to cubical specimens through three independent actuators was designed and constructed. This equipment allowed the typical stress levels and stress paths involved during rock excavation for tunnels and cuts to be represented with continuous monitoring of loads and displacements through a data acquisition system. Cubical concrete specimens were used for convenience to evaluate the equipment during the testing programme. Owing to the time consuming nature of the testing procedures, and limited time available at this stage of the programme following equipment development, little data was obtained to develop multiaxial relationship. This will be the subject of a future study now that the equipment is developed and proven. With the equipment developed and future testing, it will be possible to provide the necessary information on the following: (i) the generalization of typical uniaxial creep relationships to the multiaxial insitu conditions, (ii) time-dependent stiffness relationships for joints, and (iii) the interface interaction between rock and concrete liners.

CHAPTER 2

CHARACTERIZATION OF MATERIALS

2-1 INTRODUCTION

The two main materials usually involved in underground rock excavation work, such as tunnelling, are the rock that "loads" the tunnel and the concrete linings to resist these loads. As the rock is removed and the tunnel advances, some form of support system is required unless the rock is of high quality, which is often not the case. Both flexible and monolithic support systems can be used depending on the project, designers' preferences, and economics. It was pointed out in Chapter One that current research on the finite element method simulation of tunnelling in rock requires the characterization of both rock and concrete. In this, and the following chapter, the necessary characterization testing and how the data is incorporated within the finite element method are discussed.

2-2 CHARACTERIZATION OF MATERIALS

Usually the behaviour of materials is complex and governed by many factors including: (i) previous history and physical properties of the material; (ii) magnitude, nature, and rate of loading; and (iii) environmental conditions such as temperature, humidity, etc. The degree of complexity of course differs from material to material. For instance, steel at ordinary temperatures and stress levels may realistically be considered for design purposes to be an elastic, linear, homogenous and isotropic material. On the other hand, the behaviour of earth materials, such as rock and soil, is much more complex so that understanding their behaviour requires experimental work and statistical analysis. Mathematical expressions, or constitutive laws, are then proposed to idealize and summarize the characterization of the material. These expressions can then be readily used with the finite element method. Two basic requirements to make such expressions useful are (i) they must be simple, and (ii) they must be able to summarize the material characterization within a reasonable degree of confidence.

2-3 CHARACTERIZATION OF MASS ROCK

Rock is generally heterogeneous, anisotropic, non-linear, and always associated with great material variability. The properties of a specific formation depend primarily on: (i) properties of the mineral constituents, (ii) proportions of each mineral type, and (iii) geological history associated with it. Furthermore, if mass rock is dealt with, the insitu conditions and the geological structures associated with it must also be evaluated. The following are the marked properties of mass rock that make it difficult to characterize:

2-3-1 MATERIAL VARIABILITY

To understand the complex properties of rocks, one has to go back to geological processes and the rock cycle. The normal rock cycle starts from magma (molten rock) to igneous rock, then to sediments and sedimentary rock, followed by metamorphic processes. More than one hundred minerals have been identified. There are numerous paths through the rock cycle, with many different processes involved and a tremendous number of combinations of these minerals. The great variability of rock can be readily seen in Table 2-1, which gives the basic physical properties of some common rocks. It is clear that variability is not only observed from one type of rock to another, but noticeable ranges of characteristics are also recognized for the same type of rock. The simple classification of rock type alone is, therefore, definitively inadequate for design purposes, even with considerable engineering judgement. Insitu behaviour is even more complex since the different geological structures, and irregular processes during the formation and consolidation of rock masses, rarely result in homogeneity and isotropy. In addition the characteristics usually vary not only vertically, but also horizontally. Therefore, adequate field and laboratory measurements, including monitoring, are needed to obtain material characteristics before and during the construction process at a given site.

TABLE 2-1

BASIC PHYSICAL PROPERTIES OF SOME COMMON ROCKS

	Granite	Marble	Limestone	Sandstone
Unit Weight+ (kg/m^3)	2592-2752	2640-2864	1872-2800	1904-2688
Compressive Strenth+ (MPa)	34.5-414	55.2-186	18-193	34.5-138
Tensile Strength* (MPa)	3-5	3-9	3-6	1-3
Shear Strength+ (MPa)	25.5-33.1	8.96-44.8	5.5-24.8	2.1-20.7
Modulus of Rupture+ (MPa)	9.5-38.3	4.1-27.6	3.45-13.8	4.8-15.9
Modulus of Elasticity* (x1000 MPa)	31.3-60	50-70	30-60	13-16
Porosity* (%)	0.4-3.84	0.4-2.1	1.1-31.0	1.9-27.3

+Adapted from Kessler and Sligh (1940).

*Adapted from the International Critical Tables (1927).

2-3-2 ORTHOTROPIC PROPERTIES

All rock masses have features which make them differ greatly from ideal materials. These special features are called structures. Generally speaking, there are two types of rock structure, namely, the primary structure and the secondary structure. The primary structures are those structures formed at the same time as the rock mass itself or during its consolidation. The secondary structures are those produced during the post-consolidation period. The analysis of the arrangements and significance of these structures is very important to geotechnical engineers because the ease, method, and cost of excavation and tunnelling depend significantly on the structure of the rock.

Layering, sometimes termed stratification or bedding, is the most common and important primary structure. While it is less obvious in igneous rock, it is the most important and prominent structural characteristic of sedimentary rocks (Niagara Escarpment, for instance). Usually the sedimentary layers or beds were deposited in an essentially horizontal orientation. However, if deposited on a sloping bottom, the layers are inclined and have an angle of dip. The stratification of the rock of course results in significantly different behaviour from bed to bed.

Lateral variations in most rock masses are also observed. However, these lateral variations are more or less rather gentle and moderate, and insignificant when compared to the vertical variation due to stratification. For practical purposes, orthotropic elastic properties (transverse isotropy) are therefore often adopted to simulate bedding (Jaeger, 1972; Emery, et al, 1978). Some typical orthotropic properties of shale are given in Table 2-2.

2-3-3 DISCONTINUITIES IN ROCK FORMATIONS

Discontinuities are usually found in rock formations (excluding the evaporites). This characteristic makes rock quite different from many other materials which can be treated as continua. Special attention must be given to these discontinuities when the properties of rock are measured and used during the analysis of engineering problems. Discontinuities in rock formations are generally classified as joints, faults and crushed zones which are the results of rock rupture under stress, failure in tension, shear, or both. The main difference between a joint and a fault is that there is no significant movement parallel to the rupture surfaces at a joint, whereas large relative displacements are observed for a fault. Hence, an abrupt change in the properties of rock materials is normally expected on the sides of a fault. Crushed zones are generally larger areas of fracture caused by tectonic forces.

A discontinuity generally represents a plane or zone of weakness through the rock. In particular, joints which traverse the rock formations together with any faults or bedding, form important patterns of potential planes of structural weakness. The stress-strain behaviour of joints and discontinuity

TABLE 2-2

SHALE PROPERTIES MEASURED EXPERIMENTALLY*

ROCK PROPERTIES	RANGE	AVERAGE
Uniaxial strength perpendicular to bedding (MPa)	12.88 - 19.71	17.60
Bulk unit weight (kg/m^3)	2243 - 2435	2339
Elastic modulus parallel to bedding ($x10^6$ kPa)	4.82 - 18.60	10.06
Elastic modulus perpendicular to bedding ($x10^6$ kPa)	1.10 - 3.24	2.07
Poisson's Ratio perpendicular to the bedding	-	0.17
Poisson's Ratio parallel to the bedding	-	0.25

*From Franklin Trow Associates, 1975 (Emery, et al, 1978).

patterns, particularly time-dependency, is not well defined and requires considerable field laboratory evaluation.

Because of the various causes of joint formation, different joint patterns are observed. Shrinkage joints in sedimentary formations are usually short, discontinuous and random in pattern. However, they are commonly parallel to the bedding planes of sediments. Cooling joints in metamorphic formations are parallel and more closely spaced near the margins of the intrusion, become more widely spaced, and eventually disappear towards the core of the mass. The degree of continuity of joints affects the deformation and strength characteristics of the rock formation. Continuous joints represent pre-existing zones of weakness or failure. Formations with continuous joints will generally fail at lower values of stress than the strength of the intact rock material. On the other hand, discontinuous joints will produce a formation of greater inherent strength because complete rupture must be made through zones of intact rock material at failure.

The joint surfaces can be classified qualitatively into (i) smooth, (ii) rough, and (iii) apparently keyed as shown in Figure 2-1. A detailed description (characterization) of joint surfaces requires joint contact tests in the field or laboratory (Duncan, 1969). Unfortunately, these tests in the laboratory are uniaxial in nature and of limited applicability. The nature of joint surfaces affects (i) the stress distribution within the rock and (ii) the shear resistance

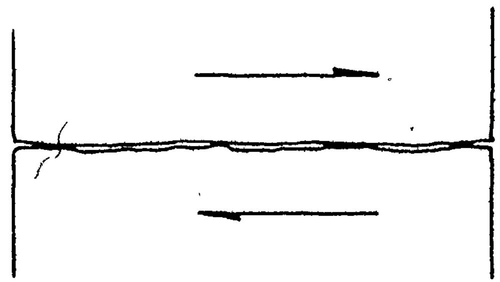

(a) SMOOTH SURFACE

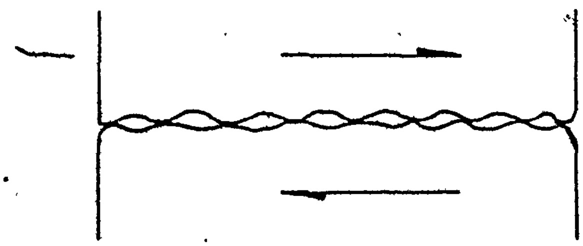

NOTE: JOINTS MAY BE INFILLED.

(b) ROUGH SURFACE

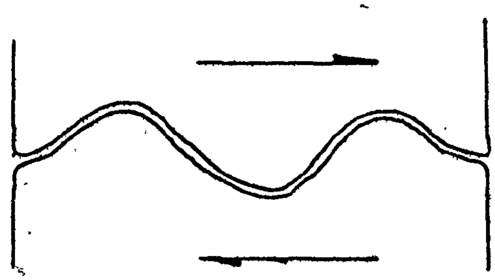

(c) APPARENTLY KEYED SURFACE

FIGURE 2-1 JOINT SURFACES.*

*After Duncan,(1969).

mobilized to resist movement along the joint. Increased roughness of the joint surfaces indicates increasing shear resistance. However, rough surfaces have less contact area, and stress concentrations and local failures may be expected if the internal stress within the rock increases, or the sliding is large enough to develop the post-peak residual shear strength.

Joints are often infilled with materials, including gauge, much different in strength from the rock material itself. Joints are therefore pre-existing planes of failure or weakness that are critical to rock engineering designs, with characteristics strongly depend on the properties of the infilled material and the orientation of the applied load in relation to the joints.

2-3-4 OTHER GEOLOGICAL AND HYDROLOGICAL FEATURES

In addition to joints, faults and crushed zones, other features, such as seams, fissures, folds and seepage conditions will also play an important role in the assessment of the behaviour of rock formations. The addition of these features to those described previously generally causes the stress-strain behaviour of rock to become even more complex and nonlinear.

2-3-5 INITIAL STATE OF STRESS

The initial state of stress of the rock formation at a site often influences its response to operations such as excavation or loading, and must generally be evaluated before a project is carried out. Since rock is a highly hysteritic material, it has a strong memory of its stress history, which is particularly important for the softer rocks such as shale. Residual stresses will remain after previously applied loads have been removed. Throughout its geological history, the rock may be subjected to over-consolidation and/or repeated changes of tectonic forces. The initial stress condition of the rock formations is therefore highly dependent on its stress history.

Figure 2-2 (a) shows the initial state of stress for an element of rock at depth z for a site with a horizontal ground surface. The vertical stress σ_z at any depth results directly from the overburden loading, while σ_x and σ_y are related to this vertical stress by the lateral stress coefficients for that depth, K_x and K_y, respectively. (It should be noted that these coefficients are usually a function of depth, and for certain conditions σ_z may not equal the overburden stress.) Assuming orthotropic properties for the rock, K_x and K_y at depth z can be taken to be equal (K), as shown in Figure 2-2 (b) and the stresses are given by (Emery, et al, 1978):

$$\left.\begin{aligned} \sigma_v &= \gamma z \\ \sigma_h &= K\sigma_v \quad \text{and} \\ \tau_{vh} &= \tau_{hv} = 0 \end{aligned}\right\} \quad (2\text{-}1)$$

where σ_v is the vertical stress on the rock at depth z,

γ is the unit weight of rock,

σ_h is the lateral or horizontal stress on the rock, and

K is the lateral stress ratio.

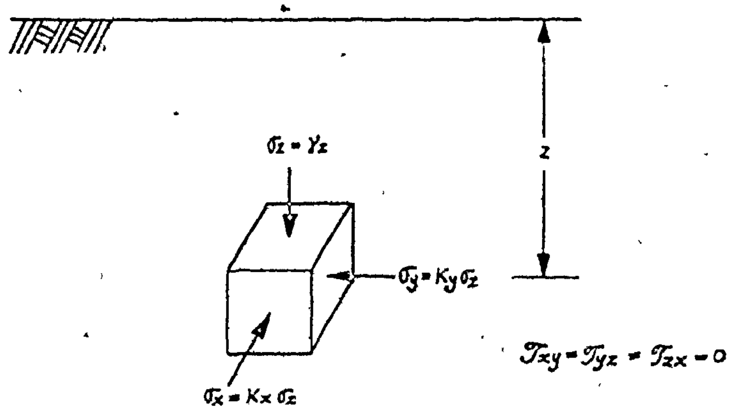

FIGURE 2-2(a) INITIAL STATE OF STRESS OF A ROCK ELEMENT AT A SITE WITH HORIZONTAL GROUND SURFACE.*
*After Desai and Abel (1972).

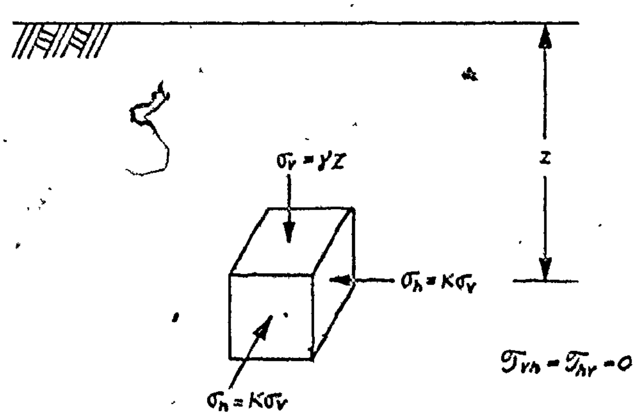

FIGURE 2-2(b) INITIAL STATE OF STRESS OF A ROCK ELEMENT AT A SITE WITH HORIZONTAL GROUND SURFACE. ASSUMING ORTHOTROPIC PROPERTY OF ROCK.†
†After Emery et al (1978).

(If water is present, these stresses and K values are in terms of effective stresses.) From the theory of elasticity, the theoretical value of K is given for the plane strain case by:

$$K = \frac{\nu}{1 - \nu} \qquad (2\text{-}2)$$

where ν is the Poisson's ratio. For a typical range of values of the Poisson's ratio for rock from 0.15 to 0.3, the values of K can be evaluated from Equation (2-2) to be between 0.18 to 0.43. However, much higher K values (see Table 2-3 covering Southern Ontario, for instance) are often reported from field measurements of high lateral stresses, indicating that the effects of tectonic history, overconsolidation and/or faults, folds, etc., must be accounted for, rather than a simple elastic approach (Emery, et al, 1978). Rock formations with high initial lateral stresses are often subject to squeezing ground conditions during excavation and tunnelling (many cases are known in Southern Ontario, for instance). This key point to tunnelling in squeezing formations will be explained in further detail in Chapter Three. It should be noted that in addition to squeezing conditions due to relaxation of high lateral stresses, swelling of soft formations can also contribute.

The shear stresses in Figure 2-2 (a) and (b) vanish only if the ground surface is horizontal and there is no surface load. However, in practice the ground surface may be sloped and/or subject to different types of loading. In either case,

TABLE 2-3

TYPICAL GROUND STRESS MEASUREMENTS FOR SOUTHERN ONTARIO*

LOCATION	ROCK TYPE	DEPTH (meters)	VERTICAL STRESS[a] (MPa)	HORIZONTAL STRESS[b]		$K = \frac{\sigma_h}{\sigma_v}$
				MAJOR (MPa)	MINOR (MPa)	
Thorold (Falmer and Lo, 1975)	Dolomite & Limestone	-13 to 15	0.301	6.61 to 14.69	5.21 to 12.07	20 to 23
Mississauga (Morton et al, 1975)	Shale	7.3 to 12.2[c]	0.172 to 0.288	up to 8.27	--	29
Pickering (Morton et al, 1975)	Shale	15.2 to 24.4	0.359 to 0.574	-1.97 to 7.45	-0.765 to 6.59	12[d]
Wesleyville (Ontario Hydro, 1975)	Limestone	below 45.7	1.08	8.27 to 13.1	6.00 to 10.62	11[d]
Niagra Falls (Ontario Hydro, 1975)	Dolomite & Shale	below 61.0	1.44	1.38 to 19.31	-1.38 to 6.21	1 to 9[d]
Scarborough (Franklin Trow Associates, 1975)	Shale	70.1	1.65	1.69[e]	1.62[e]	1

a. Bulk unit weight assumed to be 2403 kg/m^3.
b. Positive values indicate compressive stresses.
c. Below the bedrock surface.
d. Average of major and minor stresses.
e. Average of several measurements.
* From Emery et al (1978)

the shear stresses are no longer zero and must be estimated using the theory of elastic although this may not be applicable given the residual stresses.

2-3-6 NON-LINEAR AND CREEP BEHAVIOUR

It has long been observed that when a rock specimen is loaded in an uniaxial compression test, the resulting stress-strain behaviour depends on the rate of loading as illustrated in Figure 2-3. The letters t_o, t_i and t_∞ on each curve denote the relative rate of loading for the test: t_o corresponds to a very rapid loading rate (theoretically instantaneous); while t_∞ corresponds to a very slow loading rate (theoretically sustained). The non-linearity of the stress-strain curve indicates that a delayed strain is involved which is often referred to as creep strain or time-dependent strain. (A plastic strain may also be involved in each case, but this instantaneous behaviour can only be evaluated by considering non-recoverable deformation.)

The time-dependent deformation can generally be described either by a stress-relaxation law or by a creep law. For a stress-relaxation law, the dependent variable stress is expressed in terms of the independent variable time for a strain history. For a creep law, on the other hand, the strain is the time-dependent variable on a stress history. Although these two laws represent different physical meanings and offer different advantages, they have the same general purpose: to describe the time-stress-strain relationship of a material.

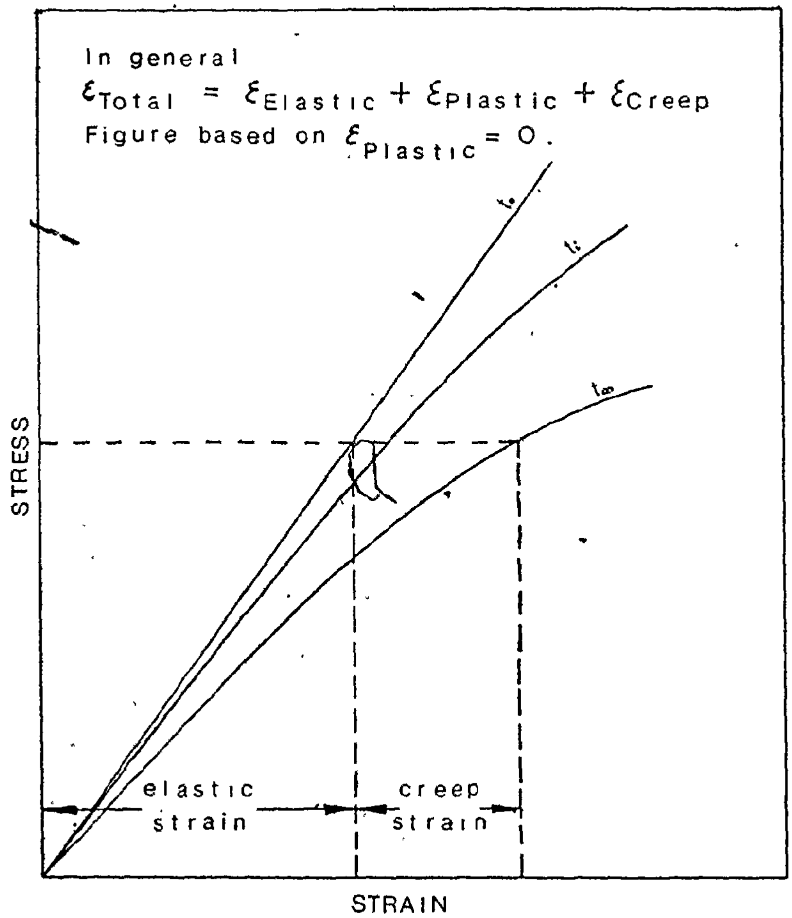

FIGURE 2-3 NON-LINEAR STRESS - STRAIN CURVES OF ROCK IN UNIAXIAL COMPRESSION TESTS (ASSUMING NO PLASTIC DEFORMATION).

In the laboratory, stress-relaxation tests and creep tests are generally used to simulate different conditions. In a stress-relaxation test, a rock specimen is brought suddenly to a state of strain, and then with this strain kept constant, the resulting time-dependent stress is measured. Similarly in a creep test, the specimen is brought suddenly to a state of stress and with this stress held constant, the time-dependent strain is measured. Step functions of strain-time or stress-time are often used to simulate the actual strain or stress history for the material.. (An example of a stress history for a specimen is shown in Figure 2-6 to be discussed later.) In practice, the uniaxial creep test is most commonly adopted for rock, soil and concrete as it is simple, accurate and can be completed in most laboratories.

Creep in geotechnology is considered to be the very slow, continuous deformation of earth materials which takes place when the state of stress is changed. This change may be due to either an increase in, or release of, internal or external stresses. Figure 2-4 shows typical schematic creep curves which are obtained by loading rock specimens under different constant uniaxial stress conditions, at constant temperature. It should be noted that while temperature is not considered herein, as shallow formations are being considered, temperature becomes an important parameter in creep relationships for greater depths where the pressure is also high (i.e. time-stress-strain-temperature relationship required). This form of creep curves is common to many engineering materials

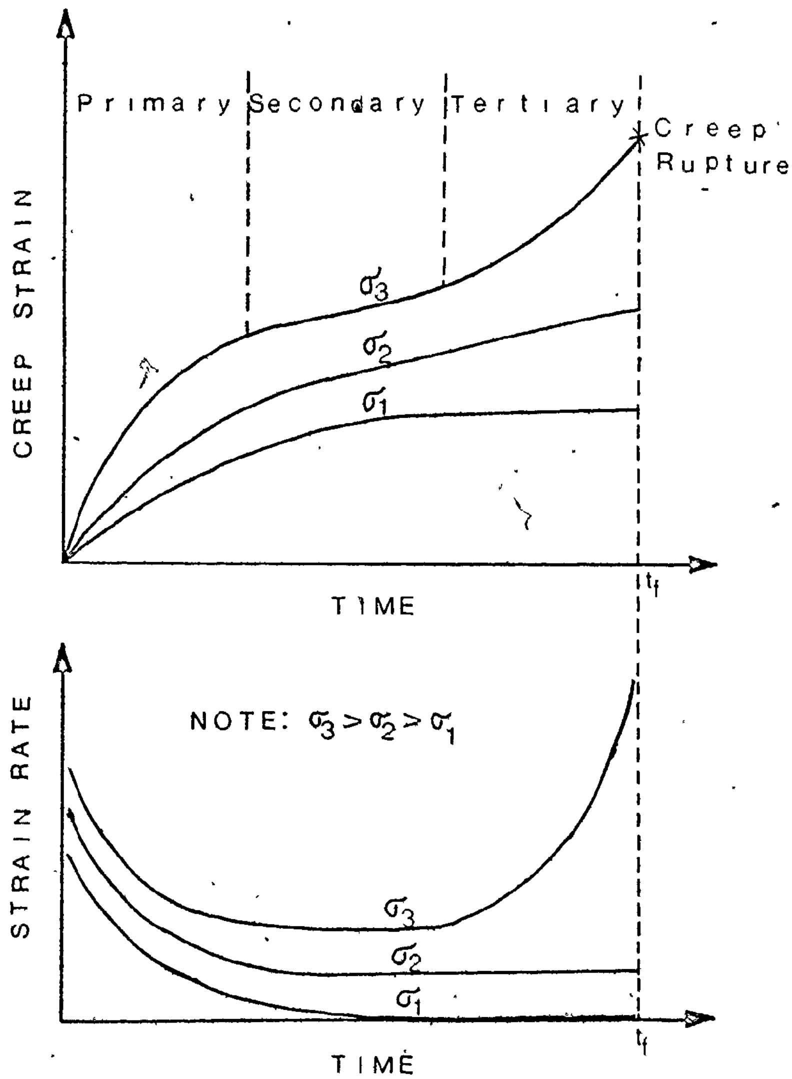

FIGURE 2-4 TYPICAL UNIAXIAL CREEP CURVES FOR ROCK SHOWING POSSIBLE BEHAVIOUR IN UNIAXIAL TESTS.

such as concrete, rock, soil, ice, plastics and steel at elevated temperatures. For instance, three stages are observed for uniaxial stress level σ_3: (i) primary or transient creep, (ii) secondary or steady state creep and, (iii) tertiary or failure creep. During the transient creep stage, the creep rate is greatest when the specimen is initially loaded, and decreases rapidly to a more or less constant creep rate. This "steady state" creep stage ends when the creep rate again increases in the final stage, followed by failure of the material. Usually, there is no clearly defined boundary between the successive stages and the existence of the three stages largely depends on stress levels, temperature, total elapsed creep time and data presentation. As shown in Figure 2-4, the specimen at uniaxial stress level σ_3 fails at time t_f, while the specimen at uniaxial stress level σ_2 is still in the steady state stage. If the stress level is low, creep may stop during the secondary stage, with no failure stage, as shown for uniaxial stress level σ_1. The effect of a temperature increase is usually an increase in creep rate as more energy is available to the creep process which is generally considered to be a rate process (i.e. thermally activated) in terms of temperature influences (Emery, 1971).

2-4 CHARACTERIZATION OF PORTLAND CEMENT CONCRETE

In many respects, concrete under load behaves in a manner similar to many brittle rock types (i.e. excluding evaporites). For this reason, research on the time-dependent behaviour of concrete often provides an insight into the corresponding behaviour of rock. In fact, for most stress-strain behaviour characterization, laboratory equipment and procedures are applicable to both rock and concrete. Some important characteristics of concrete from the point of simulating rock behaviour can be summarized as:

(1) Concrete can be cast into any shape or form. This makes it very easy and much cheaper to manufacture laboratory kit specimens in comparison to preparing rock specimens from field samples. Of course, the final development of rock creep relationships still requires tests on the actual rock involved in the project, and noting that only intact rock is being simulated at this stage.

(2) The properties of concrete depend mainly on its constitutive components (cement, admixtures, water and aggregates) that can be readily changed to simulate a range of rock behaviour. For instance, for low water to cement ratio concrete, the strength is low while the creep potential is high. Unfortunately, to a low extent, the properties of concrete also depend on many other factors, such as method and time of curing, temperature and humidity. There must be closely controlled to avoid any differences between kit specimens, and the curing time at testing must be kept constant for a test series.

(3) The elastic properties of a concrete specimen can be related to its unit weight and compressive strength by several empirical equations such as that proposed by A. Pauw (1960):

$$E_c = 0.2\ w^{1.5} \sqrt{f_c} \qquad (2\text{-}3)$$

where E_c is the modulus of elasticity in kPa,

f_c is the ultimate strength in kPa, and

w is the unit weight of concrete in kg/m^3.

Similar approaches have been used to estimate the modulus for various rocks.

(4) Concrete, like rock, is weak in tensile strength so that microcracks develop whenever the material is in tension.

(5) Unfortunately, as mentioned in (2) concrete gains strength, as the hydration process continues at a rapidly deminishing rate over a very long time period. While 28 days is often taken as maturity, this is not really the case. As the strength increases, the creep potential of concrete decreases with age and can be estimated by (Shank, 1935):

$$\delta_t = C \sqrt[r]{t} \qquad (2\text{-}4)$$

where δ_t is the specific creep strain (1×10^{-6})

t is the duration of loading in days

r is an index from creep tests, and

C is the day one creep strain (1×10^{-6}) per unit stress.

For conventional ordinary strength concrete, the value of r is about 3 and the value of C is given by:

$$C = \frac{0.5}{2.5\sqrt[5]{a}} \qquad (2\text{-}5)$$

where a is the age in days when loaded.

Another creep relationship from testing plain concrete arches, subjected to uniformly distributed loads, was developed by Straub (1930):

$$\varepsilon = 4.7 \times 10^{-10} \sigma^{1.3} t^{0.4} \qquad (2\text{-}6)$$

where ε = creep strain,

σ = the stress in kPa, and

t = time in days.

The Straub creep relationship does not consider the degree of concrete maturity like Equations (2-4) and (2-5), but, as shown in a later section, is of a form often used to describe rock creep.

(6) Concrete displays anisotropic behaviour (more specifically orthotropic, i.e. parallel and normal to the direction of casting) with a degree dependent on the aggregates, mix proportions and method of mixing and casting. For instance, when the aggregates used are of good quality and comparatively cubical in shape, and a proper method of mixing and casting is used, there is no significant degree of anisotropy in comparison with most rock. Thus, a degree of extra anisotropy can be "built in" if required to represent a specific rock formation. Irregardless, the creep, strength and modulus of elasticity for even high quality concrete were reported to be higher in specimens subjected to a load in the plane of casting compared to the normal direction (Karapetian, 1964). Some test results showing the influence of concrete anisotropy on creep are given in Figure 2-5. It is of

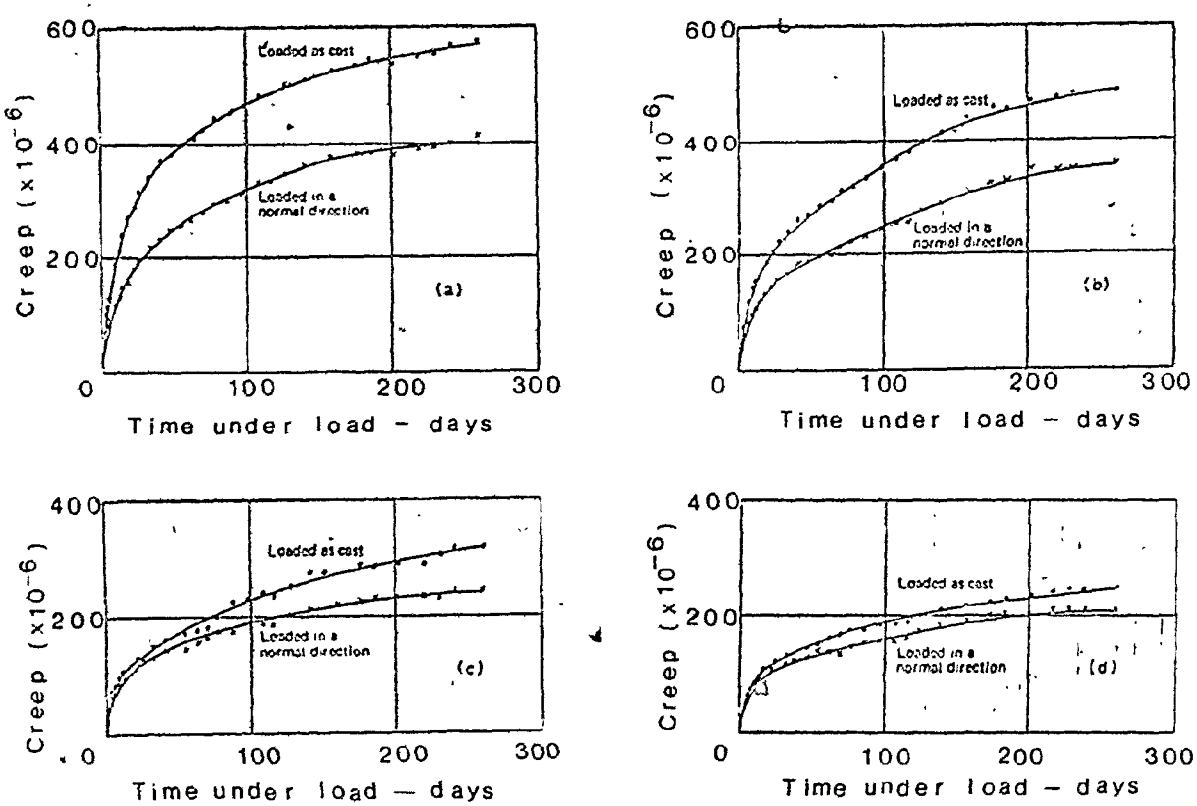

FIGURE 2 — 5 INFLUENCE OF CONCRETE ANISOTROPY ON THE CREEP OF SQUARE PRISMS UNDER A COMPRESSIVE STRESS OF 1930 kPa; PRISM SIDE: (a) 70 mm; (b) 100 mm.; (c) 150 mm.; (d) 200 mm.* *Karapetian (1964) Nevill (1970)

interest to note that the influence of anisotropy decreases with increasing specimen size, which is often observed when testing intact rocks in the laboratory. The opposite trend would of course occur if there were discontinuities present.

2-4-1 CREEP THEORIES FOR CONCRETE

A number of factors or mechanisms which affect creep have been considered to explain the creep of concrete such as: mechanical deformation; viscous flow; plastic flow; seepage of gel water; delayed elasticity; and microcracking. However, none alone can account for the behaviour when developing a fundamental creep relationship for concrete. It is clear that the actual creep must involve several of these mechanisms acting together (Neville, 1970). Because of the difficulties involved, experimentally determined creep relationships for concrete are generally used.

2-5 PREDICTION OF CREEP EFFECTS

As far as engineering applications are concerned, the prediction of creep effects is far more important than fully understanding the creep mechanism(s) involved. Three approaches are generally available to study the creep of earth and other materials: (i) the fundamental approach; (ii) the empirical approach, and (iii) the mathematical model approach.

In the fundamental, or micromechanistic approach, the creep behaviour is studied on a molecular level and is related to thermally activated processes. The creep strain rate equation is developed from the absolute reaction rate theory or rate process theory (Mitchell et al, 1968; Emery, 1978). Unfortunately, while important to understanding creep behaviour and factors involved, these strain rate equations are not adequately developed for geotechnology use at the present time.

In the empirical approach, various parameters such as strain, strain rate, stress, time elasped and temperature under controlled conditions are measured in experiments. Functional relationships among these parameters are then developed to describe and predict the creep behaviour for design applications, often using statistical design packages such as SPSS*. Alternatively, a simple tabular or graphical forms may be used in computer programs (Emery,1978). Some of the more typical empirical creep equations for rock are given in Table 2-4. Currently, most creep relationships used in rock engineering are empirical and based on uniaxial testing.

In the mathematical, or rheological model approach, an idealized model is developed to simulate the creep behaviour of actual materials. These devices are usually linear or nonlinear springs, linear dashpots (Newtonian) with a coefficient of viscosity η_i, non-linear dashpots (non-Newtonian) with creeping flow, and sometimes sliders (friction element).

---

*Statistical Package for Social Science.

TABLE 2-4

SUMMARY OF CREEP EQUATIONS AND LIMITATIONS*

ROCK CREEP EQUATION	ROCK TYPES	LIMITATIONS
$\varepsilon = K\sigma^n t^m$ (Boresi and Deere, 1963)	Rock salt	The constants (K,n,m) are given only for rock salt and for stresses ranging between 6.89 MPa and 26.53 MPa in this reference.
$\dot{\varepsilon} = A\sigma^n$ (Robertson, 1963)	Most rocks	Values of n calculated from primary creep data are given by Robertson. This equation may not be valid for all ranges of strains, i.e. does not cover the steady state creep and the tertiary creep. Also it requires experiments to define the constant A for the rock type used.
$\varepsilon = (\frac{\sigma}{E}) \ln t$ (Farmer, 1968)		This equation does not include the secondary creep. The values of n are dependent on the stress magnitude and the elastic modulus.
$\varepsilon = \varepsilon_o + g\sigma^f t + K_2\sigma \log(t+1)$ (Hobbs, 1970)	Siltstone, sandstone, shale, and limestone	The constants (g,f,K_2) are given for the four rock types for stresses ranging between 26.18 MPa and 41.34 MPa. The equation does not cover tertiary creep.
$\varepsilon = A + Bt^C + D[1-\exp(Et)]$ (Afrouz and Harvey, 1974)	Air-dried soft (coal, underclay) to medium (sandstone, limestone) rocks	The constants (A,B,C,D,E) are given for stresses ranging between 0.65 MPa and 5.72 MPa. In these equations the strain is only a function of time. The constants for the rock type tested should be determined experimentally for the stress level anticipated.
$\varepsilon = A + Bt^C + Dt^E$ (Afrouz and Harvey, 1974)	Saturated soft (coal, underclay) rocks	

*Emery et al (1978)

The mathematical description of the creep behaviour of the model is then used in the creep analysis of materials. This approach gives an overall description of the deformation response including elastic, viscous, nonviscous and plastic behaviour, or a combination of these. The advantage of the linear rheological model approach is the use of the correspondence rule for determining analytical solutions. Some of the limitations of the rheological model approach in geotechnology are: (i) The creep of most earth materials is non-linear so that the typical linear models and superposition represent only an idealized condition (Schiffman, 1959; Kondner and Krizek, 1965; Hirst and Mitchell, 1968; Scott and Ko, 1969). (ii) The success of the final solution depends on how well the response of the rheological model and the assessment of the parameters for each element represent the actual material. (iii) This approach usually works under specified conditions (for example, over a particular stress range and time interval) and does not offer a generalized representation of the creep behaviour of earth materials (Hirst and Mitchell, 1968; Scott and Ko, 1969). Based on a review of many forms of available creep relationships for earth materials, Emery (1971) concluded that the empirical approach, with consideration of the fundamental process involved, is currently the most realistic and appropriate approach in geotechnology given the complexity and nonlinear nature of these materials. This does require laboratory data (or preferably field data), but the rheological model approach is just too simplistic and not generally representative of observed behaviour.

2-5-1 CREEP UNDER VARIABLE STRESS

It is usual, and convenient, to conduct creep tests under a constant uniaxial stress condition. However, in the field, a constant stress history is rarely involved and the stress state is generally multiaxial (an exception being axi-symmetric axial loadings). Cumulative laws for creep under variable stress states are therefore needed. The two most common cumulative laws, illustrated in Figure 2-6, are the strain hardening and time hardening creep laws. In the time hardening creep law, the current strain rate depends on both the elasped time and the current stress level (i.e. $\dot{\varepsilon}_c=f(\sigma,t)$). On the other hand, in the strain hardening creep law the current strain rate depends on the current stress and strain levels (i.e. $\dot{\varepsilon}_c = f(\sigma,\varepsilon)$) (Emery, 1971; Nguyen, 1976). In both cases, a constant temperature has been assumed. It should also be noted that the strain hardening concept is often referred to as a mechanical equation of state in studying metals at elevated temperatures and stresses. For earth materials, the strain hardening creep law has been found to be realistic, and is usually adopted (Emery, 1971).

2-5-2 CREEP UNDER MULTIAXIAL STRESS STATES

Creep tests conducted in the laboratory for earth materials, such as rock, are generally uniaxial, and sometimes

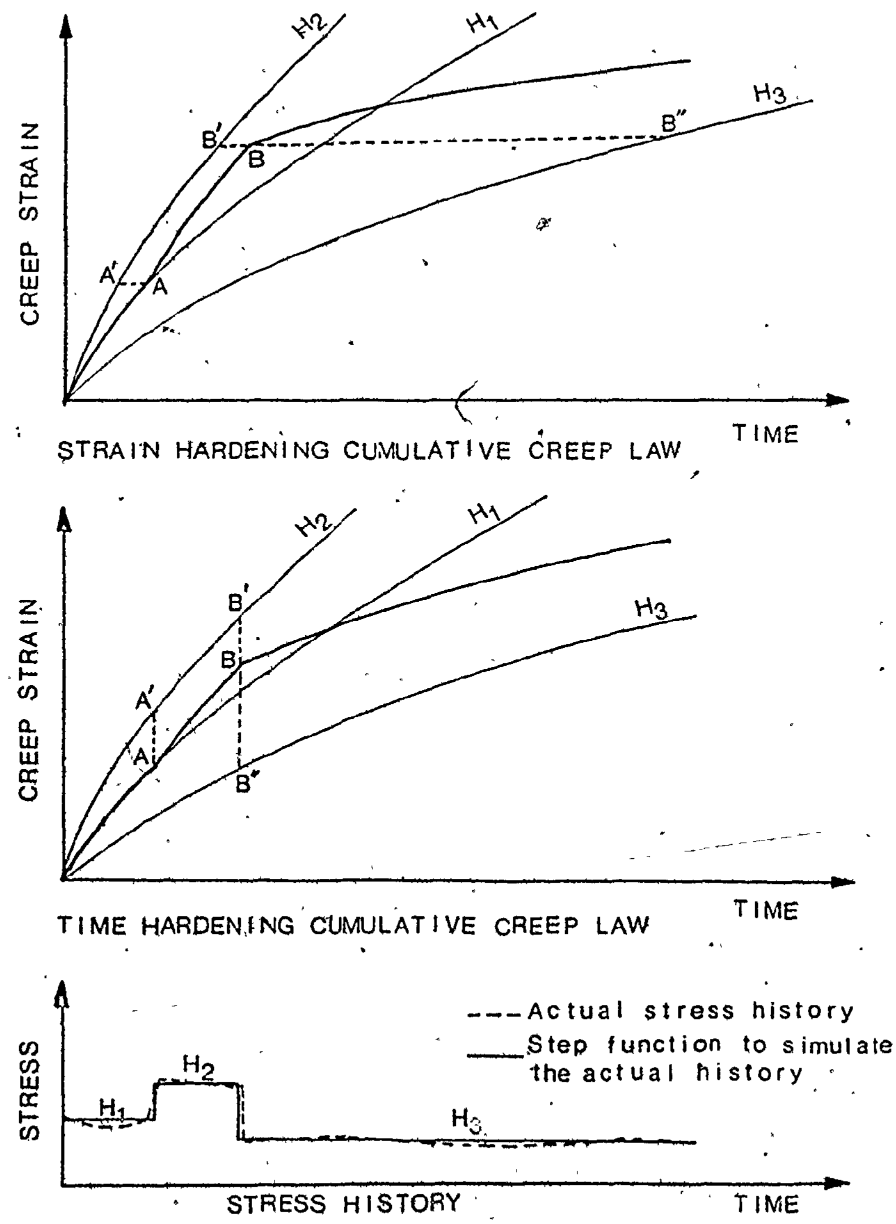

FIGURE 2-6 CUMULATIVE CREEP LAWS
After Nguyen (1976).

confined triaxial. The triaxial or multiaxial creep tests have been rarely reported in the literature. However, in practical problems involving creep such as rock excavation and tunnelling, the state of stress is usually very complicated, and the six stress components (σ_x, σ_y, σ_z, τ_{xy}, τ_{yz} and τ_{zx}) are generally involved with magnitudes dependent on past and present stress histories. Two general steps must be taken to remedy these shortcomings: (i) creep tests should be performed for both uniaxial and multiaxial stress states; and (ii) a creep theory (or theories) should be formulated yielding generalized multiaxial relationships, preferably based on the simpler uniaxial tests.

From the study of multiaxial creep behaviour of metals at elevated temperatures, and assuming similar relationships hold for incremental creep strains as for incremental plastic strains, the classical incremental plasticity (flow) law is typically adopted to give a relationship between uniaxial and multiaxial creep behaviour (Emery, 1971). The following equation is available from incremental plasticity:

$$\Delta \varepsilon_{ij}^{c} = \frac{3}{2} \frac{\Delta \varepsilon_{e}^{c}}{\sigma_e} S_{ij} \qquad (2\text{-}7)$$

where $\Delta\varepsilon_{ij}^{c}$ is the increment at creep tensor,

$\Delta\varepsilon_{e}^{c}$ is the equivalent creep strain increment,

σ_e is the equivalent stress, and

S_{ij} is the deviatoric stress tensor.

Different definitions of the equivalent stress and the equivalent strain rate for multiaxial creep laws are given in Table 2-5 and typically used in glaciology and plasticity of metals (Nguyen, 1976). The validity of this practice, and the suitabilities of adopted definitions of equivalent stress and equivalent strain rates in rock mechanics is still unknown and requires support from multiaxial creep testing. Emery (1971) and other researchers in geotechnology have often adopted Dorn's definitions.

2-6 SUMMARY

Characterization of earth materials is difficult given the problems of sampling, variability, low strengths, etc, and usually requires an elaborate laboratory and/or field programme coupled with engineering experience and judgement. This is especially true for rock where the general problem of determining appropriate properties becomes even more difficult when time-dependency is involved in the analysis (Emery et al, 1978). Further, understanding rock creep behaviour is handicapped by the fact that conventional creep tests on rock are uniaxial in nature. In contrast, considerable progress has been made in understanding the more complicated creep of concrete, and multiaxial creep tests on concrete have been reported (Gopalakrishnan, Neville, Ghali, 1969). The multiaxial creep equipment developed in this study is appropriate for most brittle materials, and as indicated in earlier sections, concrete was used in the evaluation of the test frame. Future studies will emphasize applications to rock creep and rock-concrete interfaces.

TABLE 2-5

DEFINITIONS OF EQUIVALENT STRESS AND STRAIN RATE*

SOURCE	EQUIVALENT STRESS (σ)	EQUIVALENT RATE STRAIN ($\dot{\varepsilon}$)
Nye (1953)	$\sqrt{I_2'}$	$\sqrt{J_2'}$
Lliboutry (1965)	$\sqrt{I_2'}$	$2\sqrt{J_2'}$
Meier (1960)	$(\sqrt{\frac{2}{3}})\sqrt{I_2'}$	$(\sqrt{\frac{2}{3}})\sqrt{J_2'}$
Dorn et al (1945)	$(\sqrt{3})\sqrt{I_2'}$	$(\sqrt{\frac{2}{3}})\sqrt{J_2'}$

J_2' = the second invariant of the deviatoric strain rate.

I_2' = the second invariant of the deviatoric stress.

where:

$$J_2' = \frac{1}{6}[(\dot{\varepsilon}_x - \dot{\varepsilon}_y)^2 + (\dot{\varepsilon}_y - \dot{\varepsilon}_z)^2 + (\dot{\varepsilon}_z - \dot{\varepsilon}_x)^2 + 6(\dot{\varepsilon}_{xy}{}^2 + \dot{\varepsilon}_{yz}{}^2 + \dot{\varepsilon}_{zx}{}^2)]$$

$$I_2' = \frac{1}{6}[(\sigma_x - \sigma_y)^2 + (\sigma_y - \sigma_z)^2 + (\sigma_z - \sigma_x)^2 + 6(\tau_{xy}{}^2 + \tau_{yz}{}^2 + \tau_{zx}{}^2)].$$

*From Nguyen (1976).

CHAPTER 3

EXCAVATIONS IN ROCK

3-1 INTRODUCTION

Construction in rock is common, and typically involves two main classes of problems: (i) stability of natural and artifical slopes; and (ii) excavation design for cuts and tunnels. Tunnelling is one of the most expensive and time-consuming classes of engineering construction with the rate often governed by the type of support system installed which often represents 30 to 50 percent ~~of~~ the total cost (Lane, 1975; Emery et al, 1978).

3-2 CREEP MOVEMENTS AND SQUEEZING GROUND CONDITIONS

There are many problems and engineering considerations associated with excavation in rock. Some common concerns are rock bursts, overbreak, underground water conditions, running ground conditions, squeezing ground, swelling, effects of high temperatures, dangers of gas, etc. While detailed descriptions of these problems are available, and remedial measures suggested in the literature, much current research is devoted to minimizing the influence of these problems in terms of both safety and cost. The design of tunnels in squeezing or swelling ground is an aspect of particular interest in Southern Ontario (cuts and tunnels in escarpment for instance) that is the subject of continuing research on finite element method applications to excavations at McMaster University (Emery et al, 1978; Hanafy and Emery, 1980).

Squeezing ground with tunnels is the very slow movements of weak or semiplastic rock materials into the tunnel opening that may result in significant failuros in the rock itself, or of the support system. Observations show that significant squeezing ground movements often involve a time period on the order of several weeks to several months, but periods of many years are also known such as the Niagara wheel pits. Sites with high lateral stress ratio values are typically associated with squeezing ground conditions (Southern Ontario, North Dakata, Southern Alberta for instance) (Emery et al, 1978). Discontinuities, minerology, grain size of rock materials, etc. are also important factors in predicting squeezing ground conditions, with movements across discontinuities such as bedding often being predominant. In general, softer and weak rocks which are rich in clay minerals are prone to squeezing since they are more plastic materials.

Emery et al (1978) related the squeezing ground conditions to creep movements of rock strata, and suggested that the prediction of creep is often an important design step in determining the support system to be used during the excavation of tunnels and cuts. These creep movements caused by unbalanced stresses from changes in the stress state are due to "unloading" of the "residual" lateral stresses. The stress path during excavation involves a change from the initial insitu state of stress given by Equation (2-1) to the final stress state after excavation. The final stresses for analysis are the sum of: (1) the initial stresses at the site, typically determined by field monitoring such as over-coring, and (2) the "perturbation" stresses resulting from the application of "release forces" acting around the opening to give a stress-free excavated surface (Meek, 1973; Kulhawy, 1974; Hanafy, 1976; Emery et al, 1978). It is clear that the final stress state is multiaxial, and various stress paths are involved during excavation and construction. The prediction of movements associated with squeezing ground therefore requires a multi-axial creep relationship(s) and the use of an appropriate cumulative creep law(s).

Conventionally, two construction methods are used to deal with squeezing ground condition (1) installation of a support system sufficiently strong to contain the squeezing ground (a formidable task); and/or (2) allowing controlled squeezing and then placing the final lining (a soft backing can be incorporated to allow continuing movement) when the movement stops or slows to a suitable design level. The first method is usually not only uneconomical in terms of thick liners, but also introduces design uncertainty as the loads can build-up to high levels over many years and ultimately lead to failure. The second alternative is more realistic, since once a stabilized condition is attained and monitored, there should no longer be a pontential for liner crushing. However, the time required for movement stabilization may be too long and/or the rate of tunnelling may become a critical factor, so that a combination of methods is often adopted. Current practice in squeezing ground conditions is to delay the liner placement and/or the use of a soft backing or packing, to avoid damage to the lining during the period of relatively large deformations due to creep following excavation (Emery et al, 1978; Hanafy and Emery, 1980). A suitable choice of delay time will significantly reduce the induced stresses since tests indicate that the creep rate is greatest at the time of excavation and will decrease rapidly in the primary creep stage. A viable modification, or supplement, to this method is to leave a gap between the liner and the rock, so that there is sufficient room for the potential creep movement. Some soft backing should be used to avoid voids behind the liner and for stress raisers that can result in cracking. The concrete lining-rock interface conditions often lie between two extreme cases: (1) completely rough with no slip (cast in place), and (2) smooth with some slip (precast and/or soft backing).

3-3 SWELLING ROCK CONDITION

A phenomenon very similar in response to the squeezing ground condition is the swelling ground condition. Often the "squeezing ground" is used for both the squeezing (lateral stress release) and swelling cases, or combination. Swelling ground involves an increase in volume (expansion) by one, or combinations, of processes including hydration, adsorption, absorption, expansion of pore water as a consequence of confining pressure release, etc. (shrinkage is also possible with drying and should also be considered during design). Swelling is usually a slow process which depends on the permeability of the rock and the penetration of water which is again a time-dependent process. The process gradually stabilizes since (1) the supply of pore water migrating toward the tunnel opening reduces with time and (2) a layer of "swelled materials" will shield the unexpanded materials from moisture. The potential effect of swelling is indicated by the saturation moisture content and porosities for the materials after swelling in a free swelling test. Sometimes, a clear distinction between swelling and squeezing is difficult because an introduction of even small amounts of water to some of the rock will increase the creep rate since the rock becomes more plastic. However, squeezing differs from swelling in the following ways: (1) it involves no appreciable volume change, and (2) it starts immediately after excavation, while swelling requires additional water for expansion which introduces a time delay. Nevertheless, the two conditions can be treated in a similar manner - an appropriate delay in the placement of liners with minimal moisture change to allow most of the movements to take place and thus greatly reduce the potential induced stress levels. While further research is necessary to develop effective construction methods, a very practical way to limit squeezing is to limit moisture changes during and after construction. Membranes and resin injections are being developed for this purpose.

3-4 FINITE ELEMENT METHOD FOR TUNNELLING SIMULATION

Finite element method is particularly useful, and readily adapted to earth materials, because of its capability of handling design problems associated with material characteristics such as nonlinear behaviour, residual stresses, discontinuities, large displacements, time-dependency, etc.(Zienkiewicz, 1968, 1977; Radhakrishnan and Reese, 1970; Desai, 1972; Desai and Abel, 1972; Emery, 1978). Emery et al (1978) developed a design package which incorporates a plane strain, linear displacement, triangular finite elements to simulate and analyze the design, control and monitoring of tunnel and cut excavations in rock which covered the following aspects: (1) initial stress state and lateral stress ratio K; (2) jointing and orthotropic behaviour of rock; (3) final stresses and elastic deformations immediately after excavation; (4) creep before placement of liners; and (5) interface conditions and creep behaviour of the combined rock-support-tunnel system. However, the following aspects were not included: (1) orthotropic creep behaviour of rock, and (2) time-dependency of joint movements. To study the time-dependency of rock and rock-support systems, an incremental, initial strain, finite element method was used which involved several assumptions: (1) plane strain; (2) non-homogeneous, isotropic, elastic material; (3) generalized relationship between uniaxial and multiaxial creep; (4) no volume change due to creep, i.e. Equation (2-7) is valid; and (5) no cracking due to tensile stresses but discontinuities can be simulated with a Goodman (1968) joint element. While these assumptions involve different degrees of idealizations, they were necessary because of the limited availabity of experimental data for the characterization of rock and rock-support systems, rather than the limitations of the finite element method itself. More recently, the method has been extended to simulating the advancing face and lining placement with time through an axi-symmetric finite element method approach (Hanafy and Emery, 1980). However, the rock characterization limitations still remain to be resolved.

3-5 SUMMARY

The application of finite element method to creep problems in rock mechanics requires a clear understanding of the characterization of rock, concrete liners and their interaction; in particular, the appropriate stress-strain-time relationships involved. Unfortunately, experimental research in this area has tended to lag behind the development of numerical techniques (Hanafy and Emery, 1980). While assumptions have to be made and some behaviour aspects are currently excluded from the design package because of the limited availabity of experimental data, fuller use of the finite element method is possible if more information is made available on: (1) rock-concrete interface behaviour including creep; (2) multiaxial creep relationships for rock; (3) orthotropic creep behaviour of rock, and (4) time-dependency of discontinuity movements (Emery et al, 1978; Hanafy and Emery, 1980). Design and construction of a multiaxial creep testing frame with continuous monitoring of loads and displacements through an accurate data acquisition system was, therefore, the first and probably most important experimental step to accomplish the objective of improved tunnelling simulation.

CHAPTER 4

DESIGN AND CONSTRUCTION OF A MULTIAXIAL CREEP TESTING FRAME

4-1 INTRODUCTION

This chapter deals with the design and construction of a multiaxial creep testing frame. The frame is primarily designed for testing rock and concrete, but, with minor modifications is suitable for testing other materials that exhibit creep at relatively low stress levels and ambient conditions. Further it can also serve as a multiaxial strength testing frame for these materials since two of its three independent actuators (loading pistons) can be strain or stress servo controlled in the present configuration. Future plans for the multiaxial creep testing frame include addition of servo control to the third loading direction.

4-2 BASIC REQUIREMENTS FOR CREEP TESTS

There are four basic requirements for creep tests: (1) the testing should be temperature and humidity controlled to simulate site conditions since the creep properties of most materials are dependent on environmental conditions; (2) the stresses over any cross-section of the test specimen (which are very "small-scale" compared to the site scale) should be uniformly distributed since localized stress concentrations cause microcracking and/or yielding; (3) the loading system should be capable of maintaining a constant, known stress state, with a minimum of subsequent adjustment and maintenance; and (4) the test specimens should be representative of the site materials. Any change in temperature during the test would not only affect the creep behaviour of the material, but also causes thermal expansions or contractions that can be significant in comparison to the creep strains. It is common practice to maintain the stress state constant during creep tests so that site stress changes are generally not directly simulated. Some creep tests with changing stress state (typically step form) for earth materials and concrete are given in the literature, but these are both limited and have not been applied to developing cumulative creep laws. For this reason, a multiaxial creep testing frame was required in which the principal stresses (and resulting overall stress state on any plane) could be reliably controlled over a wide range of stress paths and stress levels. Further, the testing system required automatic data monitoring and servo control so that tests could be run for extended periods. To satisfy most of these requirements, the multiaxial creep testing frame described in the following sections was developed from an existing MTS uniaxial testing frame in the Geotechnical Laboratory at McMaster University.

4-3 STRESS LEVELS AND SPECIMEN SIZE

The specimen used should be as large as possible since (1) it will be more representative in terms of site conditions such as discontinuities (these are still extremely difficult to accomodate in the laboratory); (2) larger outputs from load and deformation monitoring devices, with less "noise" due to amplification, are involved; and (3) specimen quality (plane surfaces) and ease of preparation generally improve with increasing size.

On the other hand, specimen size is limited by the maximum forces that can be generated by the creep testing frame actuators to provide the desired stress levels. The multiaxial creep testing frame constructed is equiped with a Bellofram actuator (air pressure controlled) and two MTS servo-controlled actuators (oil pressure controlled) which are capable of generating a maximum force of 20 kN and 220 kN, respectively. An example of a typical rock mechanics application illustrates the capability of the system. Suppose an excavation of a tunnel is carried out in rock 85 meters below the ground surface with a bulk unit weight of 22.55 kN/m^3. This is about the maximum depth involved in most applications of interest in civil engineering construction. The vertical stress at the depth of interest is about 1,900 kPa (Equation 2-1). Using the Bellofram actuator to generate this vertical overburden stress level limits the maximum specimen size to a 102 mm (4 in.) cube. The two MTS actuators can generate maximum lateral stresses of 21,300 kPa, corresponding to a maximum lateral stress ratio of 11. This is considered the upper limit on lateral stress ratios from monitoring and field construction experience. It should be noted that while the available actuators and auxiliary parts were suitable for the stresses of interest, there were severe financial and time constraints in developing the overall system. For this reason, further development work continues.

4-4 DESIGN OF LOADING PLATENS

The overall multiaxial creep testing system is shown in Figure 4-1 where the cubical specimen is loaded through six stiff polished steel platens as shown in Figure 4-2. A loading cap, 76.20 mm (3 in.) in diameter, 12.70 mm ($\frac{1}{2}$ in.)* thick, and with a curvature of 38.10 mm ($1\frac{1}{2}$ in.) at the centre, is bolted to each steel platen. Two essential elements were considered in the design of these loading platens, i.e. the size and thickness. Each steel platen is square, with a width slightly less than that of the specimen to allow a gap between the adjacent platens. The function of these gaps is to ensure that any lateral squeezing or swelling of the specimen is not restricted by load transfer between any adjacent platens. However,

---

*All construction machining drawings were completed in imperial units.

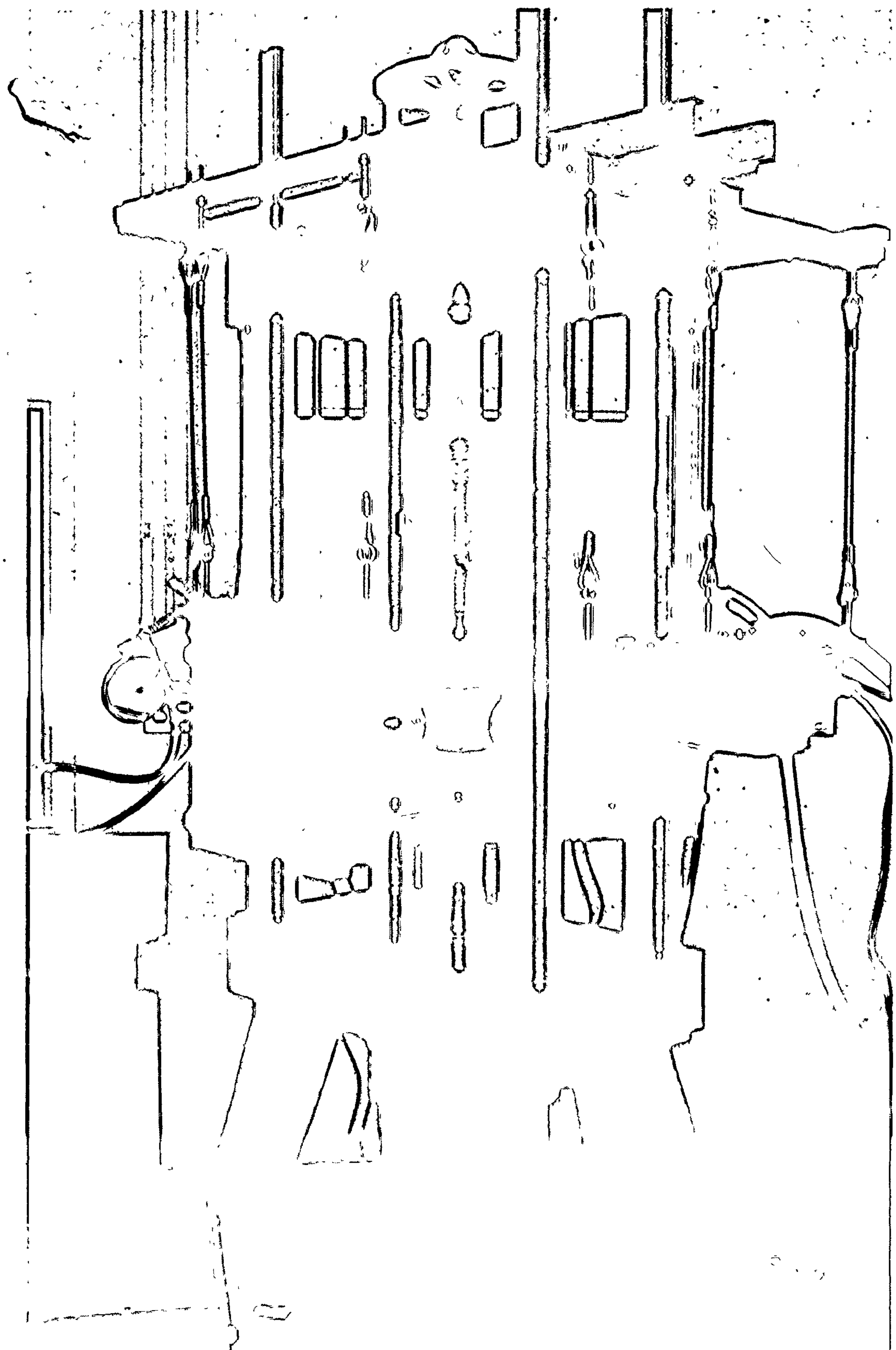

FIGURE 4–1 MULTIAXIAL CREEP TESTING FRAME.

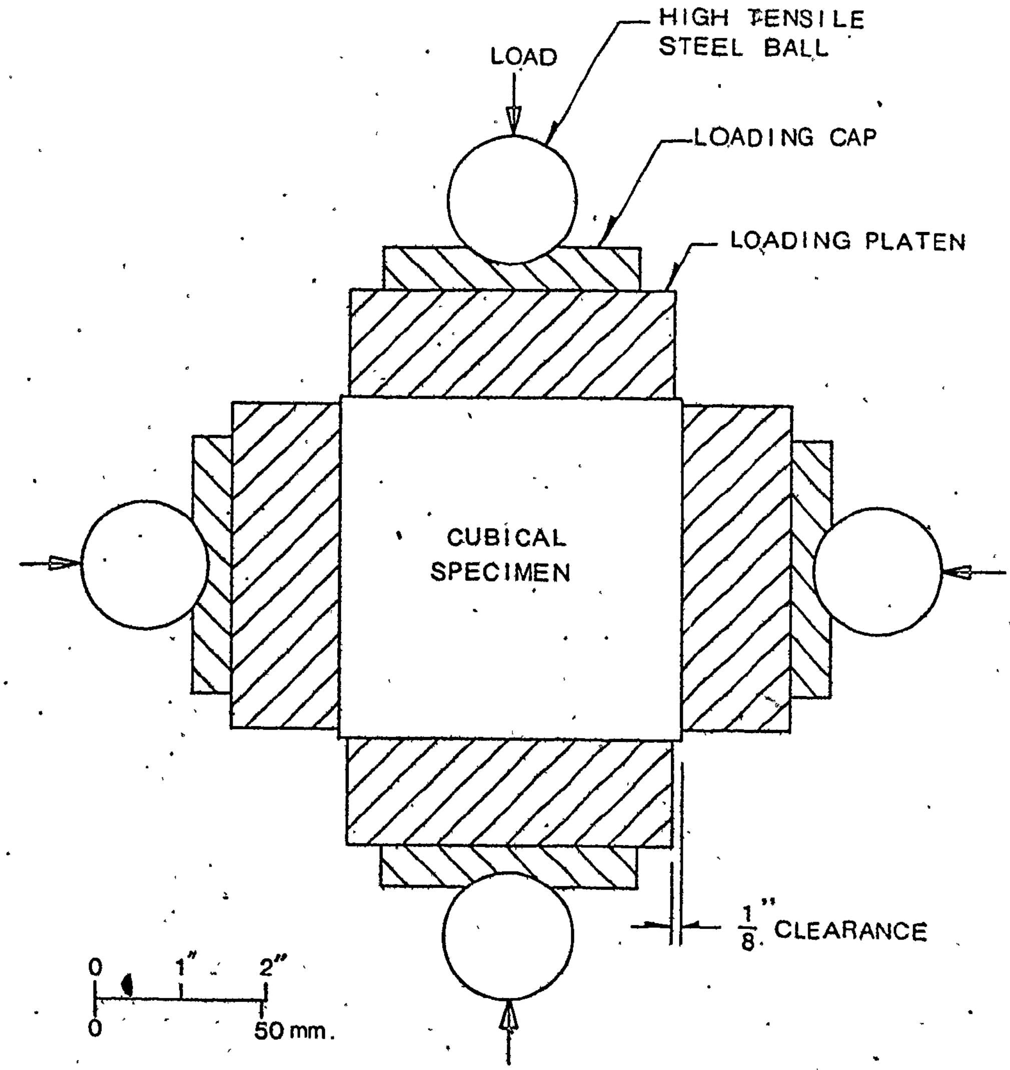

FIGURE 4-2 ARRANGEMENT OF SPECIMEN AND LOADING PLATENS.

gaps have been minimized so that the platens cover as much of the specimen as possible, and a fairly uniform normal stress is developed over the specimen face. To optimize the objective of minimizing platen interference while producing a uniform loading, the total maximum lateral strain (both elastic and creep) of softer rock materials under an uniaxial compressive stress of 21,300 kPa was estimated using Hobb's creep equation for shale (1970):

$$\varepsilon = \varepsilon_0 + 1.98 \times 10^{-9} t + 7.56 \times 10^{-9} \sigma \log(t+1) \quad (4\text{-}1)$$

where ε is the total strain (elastic and creep),

t is the time in minutes,

σ is the stress in kPa, and

ε_0 is the elastic strain, σ/E.

Referring to the typical measured properties of shale in Table 2-2, the rock is more compressible when loaded perpendicular to the bedding. The value of the elastic modulus, E, is taken as 1.0×10^6 kPa, at the lower end of the appropriate modulus range (1.10×10^6 kPa to 3.24×10^6 kPa). For a uniaxial stress, σ, of 21,300 kPa and test duration, t, of 6 months (260,000 minutes), a maximum total strain of 2.27×10^{-2} is obtained from Equation (4-1), giving a maximum total deformation of 2.32 mm for the 102 mm cubical specimen. Also softer rocks (mudstone, for instance) may be tested in the future. The width of the loading platens was, therefore, selected to be

96.84 mm ($3\frac{13}{16}$ in.), leaving a gap of 2.38 mm on each side of the platen. This clearance was checked for concrete specimens by making use of Equations (2-3) and (2-6). For ordinary concrete with a bulk unit weight of 2,300 kg/m^3, compressive strength of 30,000 kPa, and creep test duration of six months, a total deformation of 0.74 mm is expected, which is much less critical.

When the specimen is loaded, the loading platen will be bent somewhat, depending on its stiffness and the magnitude of loading. While a detailed stress-strain analysis of the platen under loading is possible, a simplified, but conservative, method was adopted to check the design by assuming that the platen is centrally loaded to 220 kN and simply supported on its four edges. The maximum deflection at the centre of the square platen can then be evaluated from plate theory as:

$$w_{max} \doteq \frac{4PS^2}{\pi^4 D} \sum_{m=1,3,..}^{\infty} \sum_{n=1,3,..}^{\infty} \frac{\sin(m\pi/2)\,\sin(n\pi/2)}{(m^2+n^2)^2} \qquad (4\text{-}2)$$

where P is the concentrated load at the centre,

S is the width of the square platen,

D is the stiffness of the platen = $\frac{Et^3}{12(1-\nu^2)}$,

t is the thickness of the platen, and

ν is the Poisson's ratio of steel.

On expanding, Equation (4-2) is simplied to:

$$w_{max} = 0.095 \frac{PS^2}{D} \qquad (4\text{-}3)$$

For a 96.84 mm square steel platen of thickness 31.75 mm ($1\frac{1}{4}$ in.), the maximum deflection, w_{max}, is calculated to be 0.34 mm, assuming that the elastic modulus of steel is 200 x 10^6 kPa and Poisson's ratio is 0.27. Since the maximum elastic modulus of shale in Table 2-2 is 18.6 x 10^6 kPa, the minimum elastic deformation of the specimen when loaded is expected to be 0.12 mm.

From the above analysis, the maximum deflection of the platen and the elastic deformation of the rock are of the same order. Further, it should be pointed out that this approach is very conservative. The actual deflection of the platen will be much smaller since: (1) the actual stress distribution is fairly uniform from the loading; and (2) the use of the loading cap (12.70 mm thickness) on top of the platen increases the platen stiffness and makes the load even more uniformly distributed over the platen. From the above consideration, it is concluded that the platen design is adequate to provide a fairly uniform stress distribution over the surface of the test specimen.

4-5 GENERAL DESCRIPTION OF THE MULTIAXIAL CREEP TESTING FRAME

The multiaxial creep testing frame (Figure 4-1) is essentially made up of three mutually perpendicular uniaxial loading frames. The vertical frame is a MTS stiff, universal testing frame with a MTS hydraulic actuator mounted at the bottom and a load cell installed at the top. The load applied to the specimen causes it to react against the load cell with the resulting output signal transmitted to the control panel SERVAC where it is compared to the pre-programmed command, and the necessary compensating signal sent to the servo valve. This servo valve controls the amount of hydraulic fluid entering the actuator via flexible hoses to and from the hydraulic power supply located remotely in the basement. Hence, a fairly constant load can be maintained throughout the test propgram (i.e. load controlled test).

A linear variable differential transducer (LVDT) is mounted in the lower part of the actuator. The function of the LVDT is to sense the position of the actuator piston rod. Thus, the output of the LVDT represents the displacement of the specimen under the loading condition. This LVDT signal may also be selected as the feedback signal which controls the system (i.e. displacement controlled test).

A key programmable data acquisition system (Esterline Angus Model) is used to display the output signal of the load cell and the LVDT by means of a digital printer. If desired, other output devices which are more compatible with computers such as magnetic tape recorders, paper tape perforators or data telemetry interfaces may be used. The data acquisition system can scan, measure, collect, identify and record electrical signals over a one second time interval for 248 channels (analog to digital conversion). The precision of the output to the digital printer is up to 8 significant figures. This system proved to be very convenient and accurate, while reducing monitoring and data reduction time.

The interaction and the function of individual parts of the load frame and the electronic control system are illustrated schematically in Figure 4-3. (More detailed descriptions of each part are available in the operation and instruction manuals supplied by manufacturers.)

One of the horizontal testing frames is essentially idential to the vertical frame described in previous sections (Figures 4-1 and 4-4). However, because of technical problems still being resolved, probably related to the lack of a separate strain gauge circuit for feedback loop from the load monitoring loop, only the LVDT feedback signal could be selected to control this horizontal MTS actuator. For this reason, the pre-programmed command of the LVDT control was set to a value such that the feedback signal was less than the pre-programmed command throughout the test program. The pressure in the MTS actuator was then restricted to one of three pump pressure conditions: OFF (zero pressure), LOW (690 kPa - 14.3 $\pm$ 0.12 kN*), and HIGH (20.7 MPa - 175.6 $\pm$ 0.2 kN*), as selected on the control unit. Through this temporary method to expedite experimental work, the two high lateral pressures could be set.

*These figures were calculated from experimental test data.

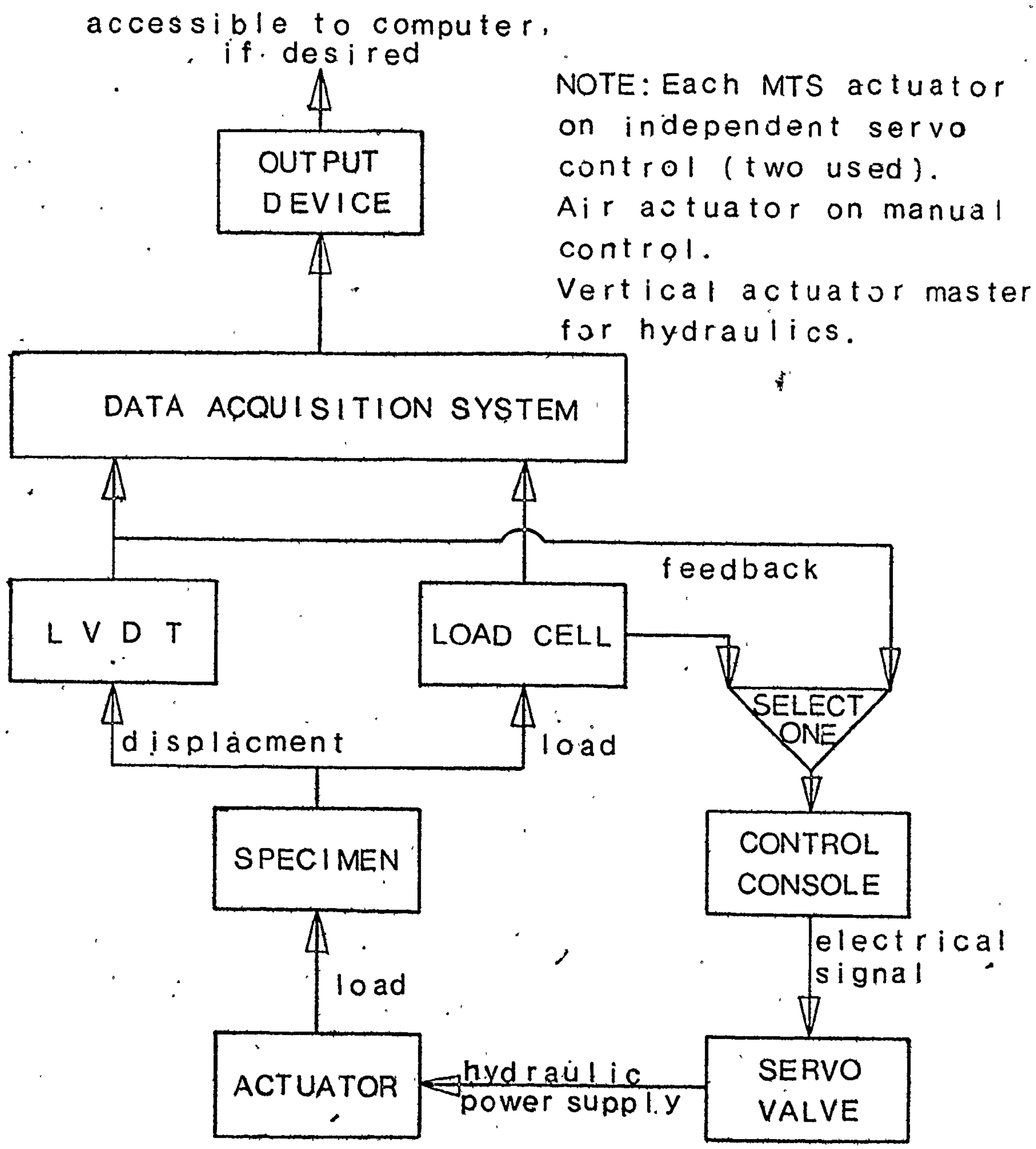

FIGURE 4-3 FUNCTIONAL ELEMENTS OF LOAD FRAME AND ELECTRONIC CONTROL SYSTEM.

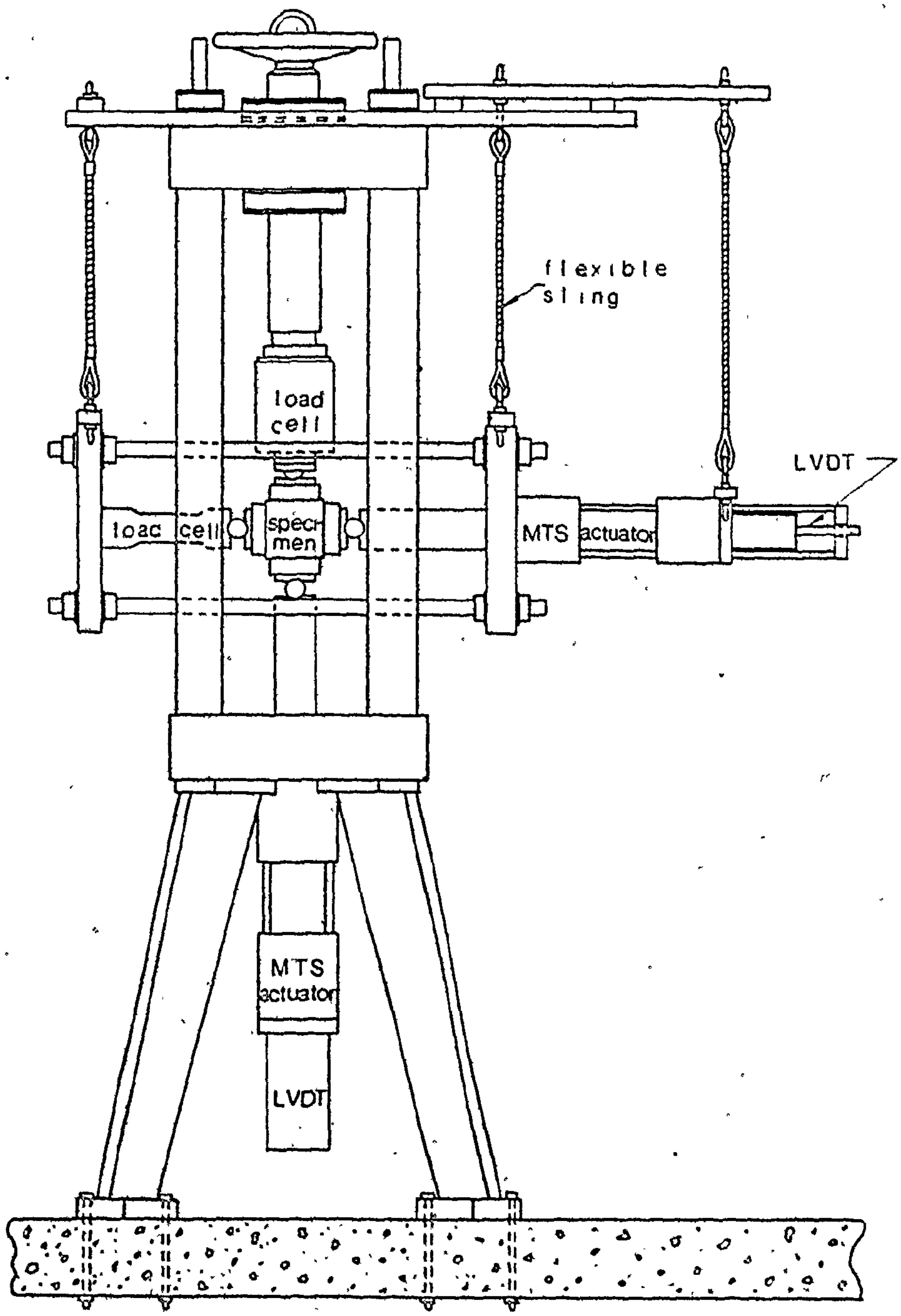

FIGURE 4—4 SECTION OF MULTIAXIAL TESTING FRAME, SHOWING VERTICAL AND HORIZONTAL MTS LOAD FRAMES

A simple, air pressure controlled Bellofram actuator was used in the third axis (Figures 4-1 and 4-5), representing the vertical stress direction (i.e. two MTS actuators represent lateral stress directions). The force generated by this actuator was adjusted by manually varying the air pressure. An LVDT clamped firmly to the lower stiff bearing plate of the vertical frame was used to measure the specimen deformation in this direction during trial tests. This did not prove successful and modifications to measure directly across the loading platens are recommended.

The two horizontal load frames are suspended by pairs of adjustable flexible slings from the upper supporting frame as shown in Figures 4-1, 4-4 and 4-5. The footings of the multiaxial testing frame are bolted firmly to the concrete floor slab so that any rocking or vibration of the system is minimized (Figures 4-4 and 4-5).

Ball and socket bearings are used with the loading platens on six sides of the specimen. Each ball is made of high tensile steel with a diameter of 38.10 mm (1 $\frac{1}{2}$ in.), and is socketed between the loading cap and a cap attached to the load cell or actuator (Figures 4-2, 4-4 and 4-5). Thus, each loading platen is able to rotate freely about the ball. The functions of this ball and socket feature are (1) to protect the load cells since they have a limited moment capacity, and (2) to permit the specimen to orient itself in the most stable position during testing.

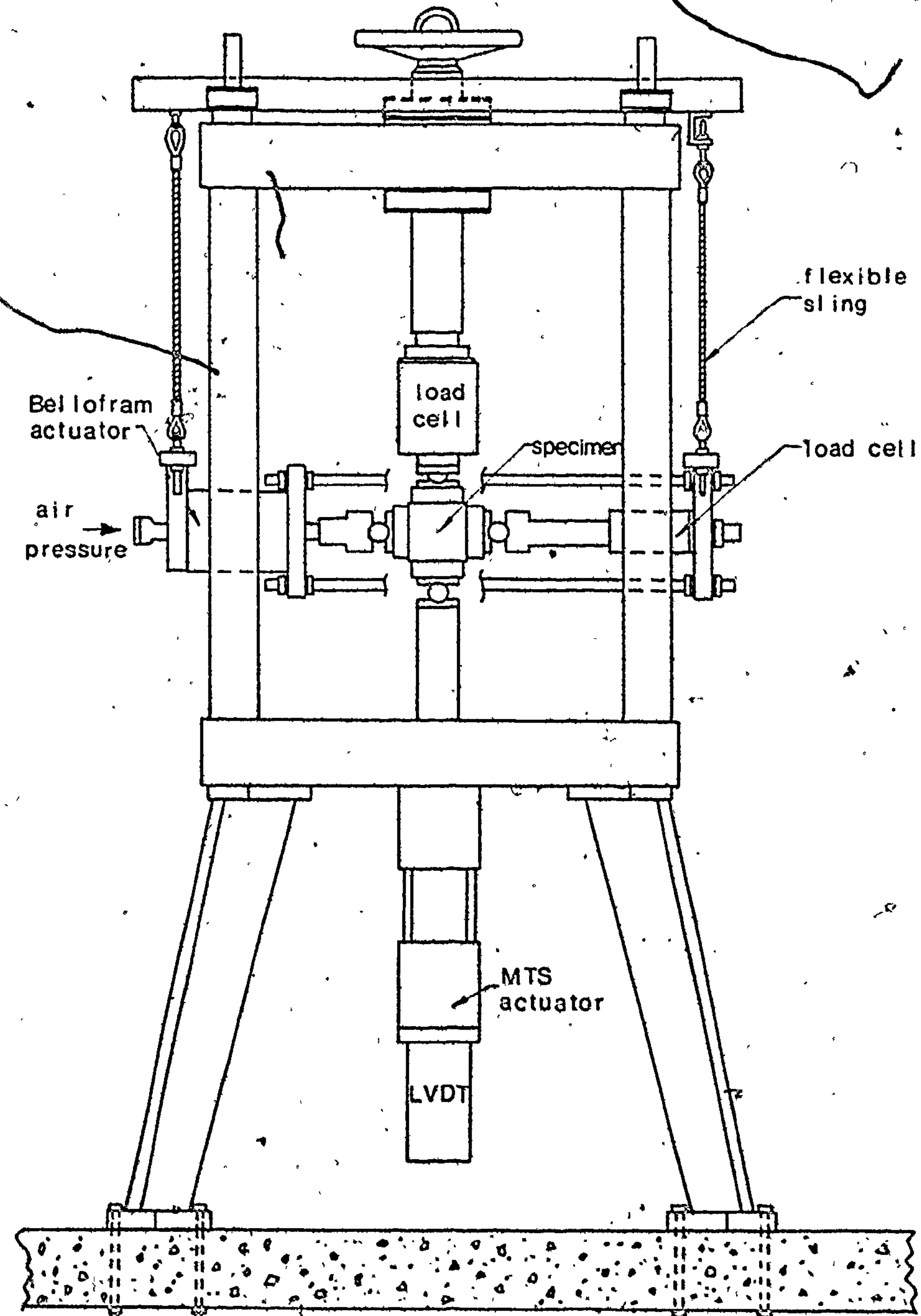

FIGURE 4—5 SECTION OF MULTIAXIAL TESTING FRAME, SHOWING VERTICAL MTS AND HORIZONTAL BELLOFRAM LOAD FRAMES.

Schematic drawings and photographs showing the arrangement and functions of individual parts of the multiaxial creep testing frame are illustrated in Figure 4-4 to Figure 4-10. The design of the 440 kN load cell and structural considerations for the design of the steel rods and stiff bearing plates of the two horizontal load frames are given in later sections 4-7 to 4-9.

4-6 SPECIAL FEATURES OF THE MULTIAXIAL CREEP TESTING FRAME

Two important, and special, features were involved in the design of the multiaxial testing frame: (1) the use of servo-controlled MTS actuators so that load or deformation controlled creep and strength tests (including post failure) can be completed, and (2) the use of a floating system for the two horizontal load frames to avoid shear transfer. These features are believed to provide an important first step in resolving technical problems generally experienced during multiaxial creep testing.

4-6-1 CONSTANT STRESS

The most important problem in multiaxial creep testing is provision of a constant, or known changing, stress condition throughout the test. In most creep tests, load is applied to the specimen through a large spring by four high tensile steel rods anchored over two stiff bearing platens. To maintain an approximately constant stress over the specimen, the apparatus

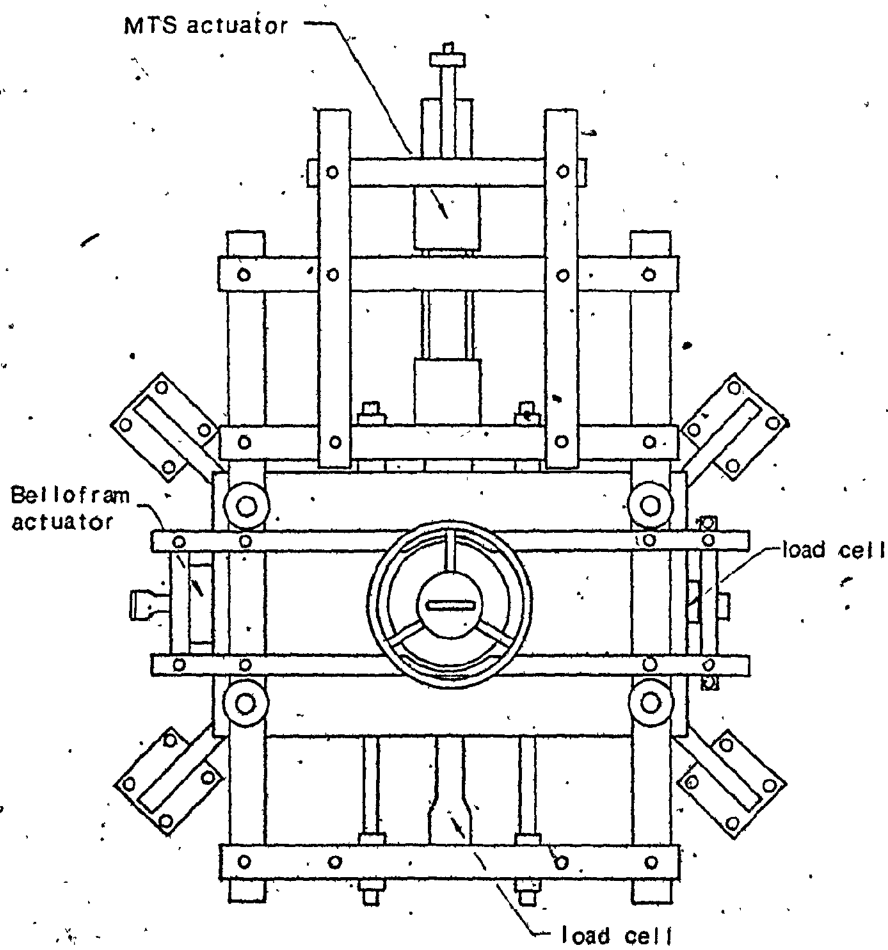

FIGURE 4-6 TOP VIEW OF THE MULTIAXIAL TESTING FRAME.

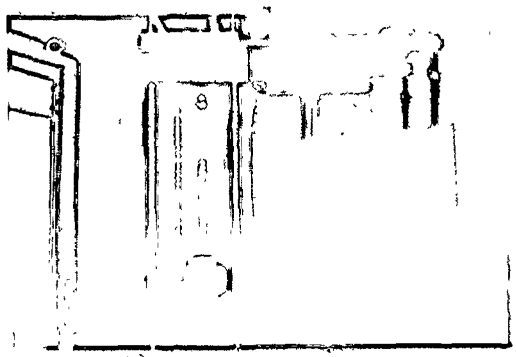

FIGURE 4-7 SPECIMEN BIAXIALLY LOADED WITH THE VERTICAL AND HORIZONTAL MTS ACTUATORS.

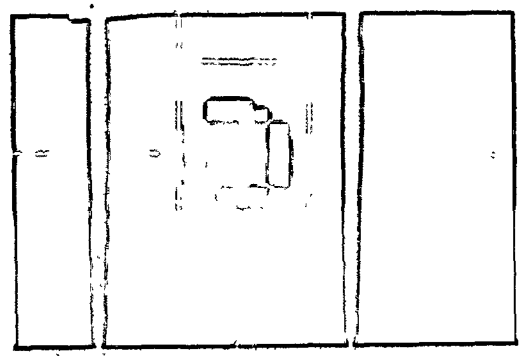

FIGURE 4-8 SPECIMEN BIAXIALLY LOADED WITH THE VERTICAL AND HORIZONTAL MTS ACTUATORS CLOSE VIEW

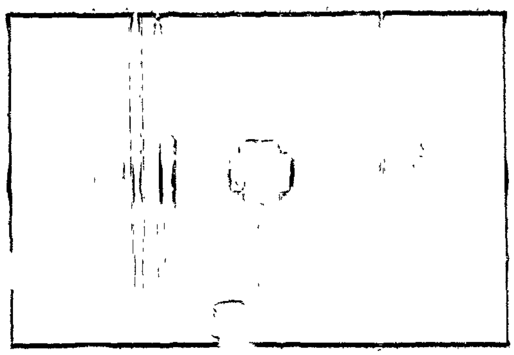

FIGURE 4-9 SPECIMEN BIAXIALLY LOADED WITH THE VERTICAL MTS AND HORIZONTAL BELLOFRAM ACTUATORS

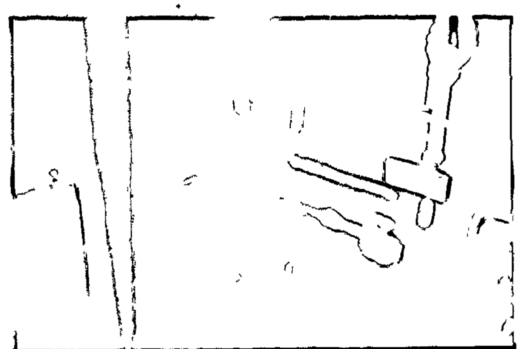

FIGURE 4-10 SPECIMEN TRIAXIALLY LOADED

has to be adjusted manually from time to time. The use of a servo-controlled MTS actuator eliminates this inconvenience and provides a very constant stress throughout the test because of the electrical feedback signal used to control the applied load. This can also be used to undertake other stress paths. Experimental data show that the load generated by the vertical MTS actuator fluctuates only slightly and completes one cycle per day with an average standard deviation of only ± 0.3 kN at a mean value of 166 kN. For the horizontal MTS actuator, comparable values were ± 0.2 kN at a mean value of 175.6 kN. Probably, this insignificant fluctuation and cycling pattern of load is partially due to fluctuation of electrical power in the building. Another advantage of using the MTS servo-valve actuator is that a nearly instantaneous loading is possible, and the unloading operation to a desired stress level can be achieved within a very short time (less than 10 seconds). The multiaxial loading of the sample and establishing the initial conditions required less than 2 minutes, even during the trial tests for gaining confidence. (See Chapter 5 for details.)

4-6-2 FLOATING SYSTEM

Since the two horizontal load frames are suspended by pairs of flexible slings from the upper supporting frame, they are free to move vertically and horizontally when the specimen deforms so that physical constraints and shear transfer are largely eliminated. If a rigid system is used instead of a floating one, the compressive reactions in the tie-rods impose forces in addition to the shear transfer due to creep movements.

4-7 DESIGN OF 440 kN LOAD CELL

The design steps for the 440 kN load cell used with the horizontal MTS actuator are summarized in this section.

MATERIAL: C1020 cold finished steel

Yield strength: 440 MPa

Modulus of elasticity, E: 200,000 MPa

Elongation per 50 mm: 20%

Hardness: 156

STRAIN GAUGES:

EA-06-125-BZ-350

Grid length: 0.15

Allowable strain: 1200×10^{-6}

DESIGN

Use: 76.20 mm (3 in.) diameter rod.

Outer diameter after machining: 57.15 mm ($2\frac{1}{4}$ in.).

Allowable stress for the strain gauges:

$$= E\epsilon$$

$$= 200{,}000 \text{ MPa} \times 1200 \times 10^{-6}$$

$$= 240 \text{ MPa } (< 0.54 f_y).$$

For 440 kN load cell

$$\text{Area required} = \frac{1}{4}\pi(57.15^2 - D^2) = \frac{440 \text{ kN}}{0.24 \text{ kN/mm}^2}$$

Therefore, inside diameter required, D equals 30.53 mm,

Use 30.16 mm ($1\frac{3}{16}$ in.).

See Figure 4-11 for detailed dimensions.

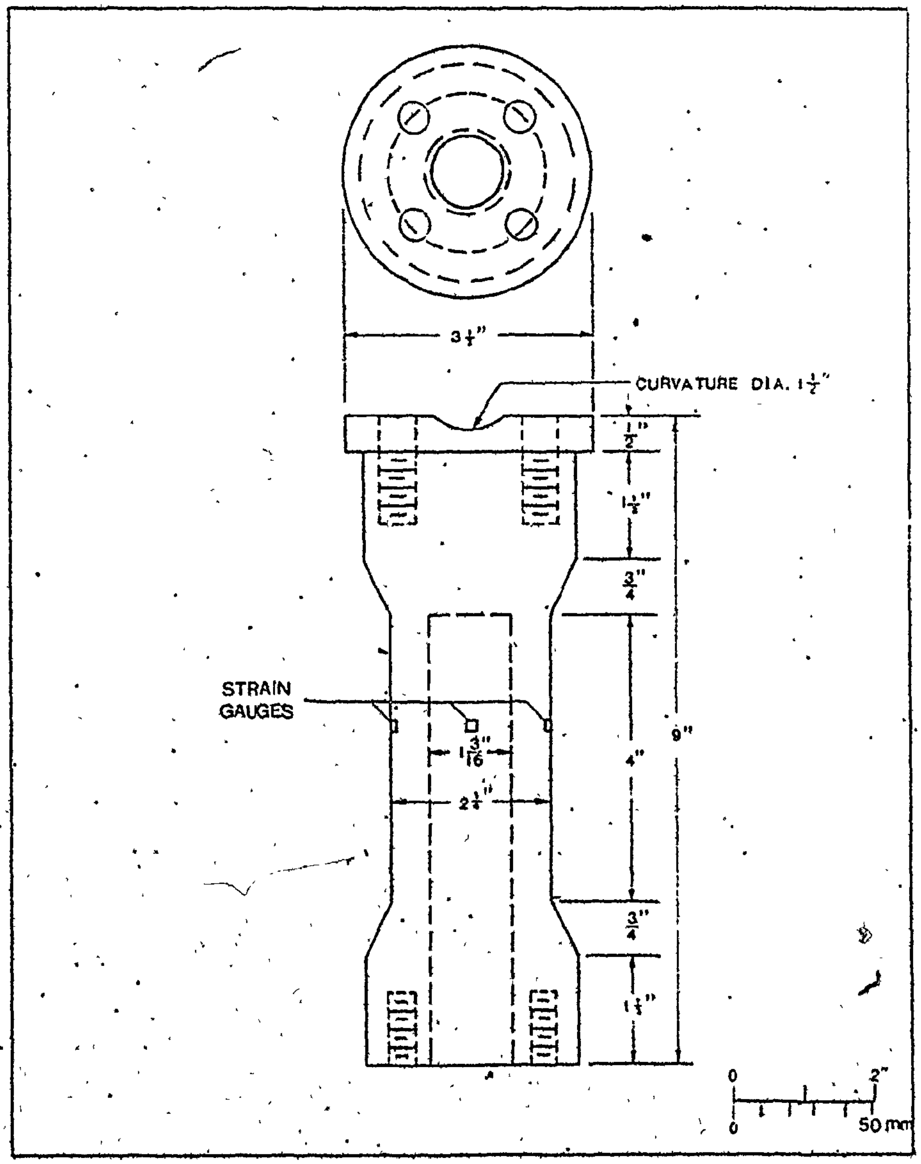

FIGURE 4-11 DESIGN OF THE 440 KN LOAD CELL.

4-8 DESIGN OF TIE RODS

The design steps for the tie rods used with the horizontal MTS actuator and Bellofram actuator are summarized in this section.

<u>MATERIAL:</u> Yield strength, f_y: 440 MPa
Tensile strength: 517 MPa
Elongation per 50 mm: 20%
Hardness: 156

<u>220 kN ACTUATOR</u>

Assuming only two of the four tie rods to carry the full load of 220 kN, the maximum load carried by one single rod will be 110 kN.

$$\text{Allowable stress} = 0.61\ f_y$$
$$= 0.61 \times 440$$
$$= 268\ \text{MPa}$$

Therefore, the required area

$$= \frac{110{,}000\ \text{N}}{268\ \text{N}/\text{mm}^2}$$
$$= 410\ \text{mm}^2,$$

and the diameter of rod required

$$= \sqrt{4 \times 410/\pi}$$
$$= 22.85\ \text{mm}.$$

Use 28.58 mm ($1\frac{1}{8}$ in.) diameter rod to give an effective area greater than 410 mm^2 after being threaded.

20 kN BELLOFRAM ACTUATOR

The maximum load carried by one single rod is 10 kN. Hence, the required area of the rod

$$= \frac{10,000 \text{ N}}{268 \text{ N/}_{\text{mm}^2}}$$

$$= 37.31 \text{ mm}^2$$

The diameter of the rod

$$= \sqrt{4 \times 37.31 / \pi}$$

$$= 6.89 \text{ mm.}$$

Use 15.88 mm ($\frac{5}{8}$ in.) diameter rod to give an effective area much greater than 37.31 mm^2 after being threaded. The use of larger size rods gives a more rigid and higher bending resisting frame since the weights of the Bellofram actuator and the load cell provide a bending load on the frame.

4-9 DESIGN OF STIFF BEARING PLATES FOR THE TWO HORIZONTAL LOAD FRAMES

Two stiff bearing plates are used in the construction of each horizontal frame. The function of these plates is to provide anchorage for the actuator, load cell and the high tensile steel rods. The necessary size and thickness of the plates were the two essential considerations during their design. The sizes of these plates were essentially determined by the size of specimen, loading platens, and the steel tie-rods, as well as the geometric specification of the actuator so that sufficient room is provided for the insertion of the specimen without obstruction among the three mutually perpendicular testing frames. It was found that 355.60 mm (14 in.) and 234.95 mm (9 $\frac{1}{4}$ in.) plates would be suitable for the MTS actuator and Bellofram actuator, respectively. The dimensions of these bearing plates after machining are given in Figures 4-12 and 4-13. These bearing plates were made thick enough to provide strength against failure and excess bending. While a detailed stress-strain analysis of these perforated plates is possible, a much simpler approach was adapted. Consider the bearing plate which is attached to the 220 kN MTS actuator in Figure 4-12. Instead of analyzing the whole plate, a beam, which is centrally loaded with half of the maximum force (i.e. 110 kN) generated by the actuator and simply supported 254.00 mm (10 in.) apart, is examined. For initial design, the effective width of the beam was assumed to be 107.95 mm (4 $\frac{1}{4}$ in.) (the distance from the edge of the bearing plate to the nearest bolt hole). The determination of the depth of the beam, d, will then give the required thickness of the bearing plate. The specification for the bearing plate was

ASTM A-283-D Steel

Modulus of elasticity, E: 200,000 MPa

Yield strength, f_y: 200 MPa (N/mm^2).

$$\text{Maximum bending moment, } M = \frac{1}{2} \times 110{,}000 \text{ N} \times 127 \text{ mm}$$

$$= 7.0 \times 10^6 \text{ N-mm}$$

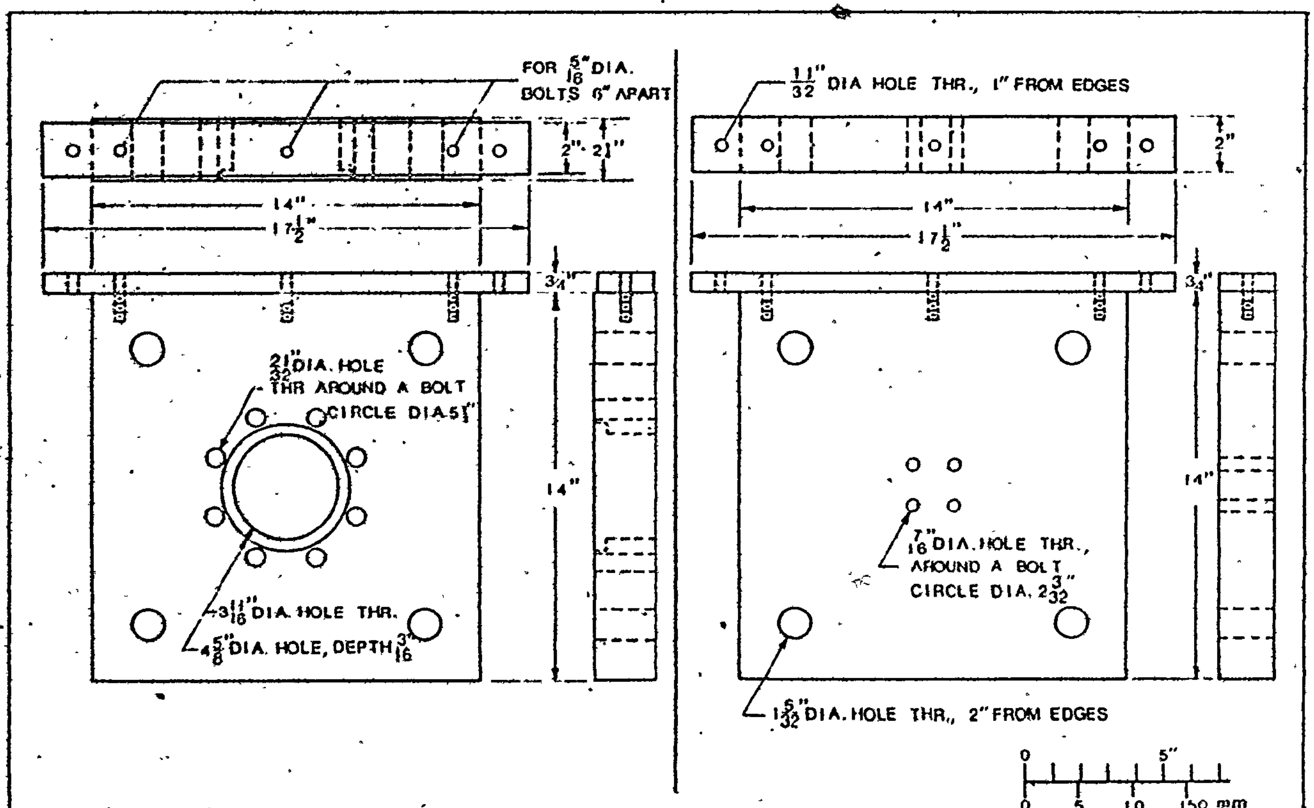

FIGURE 4-12 DESIGN OF TWO STIFF BEARING PLATES OF THE HORIZONTAL LOAD FRAME WITH 220 KN MTS ACTUATOR

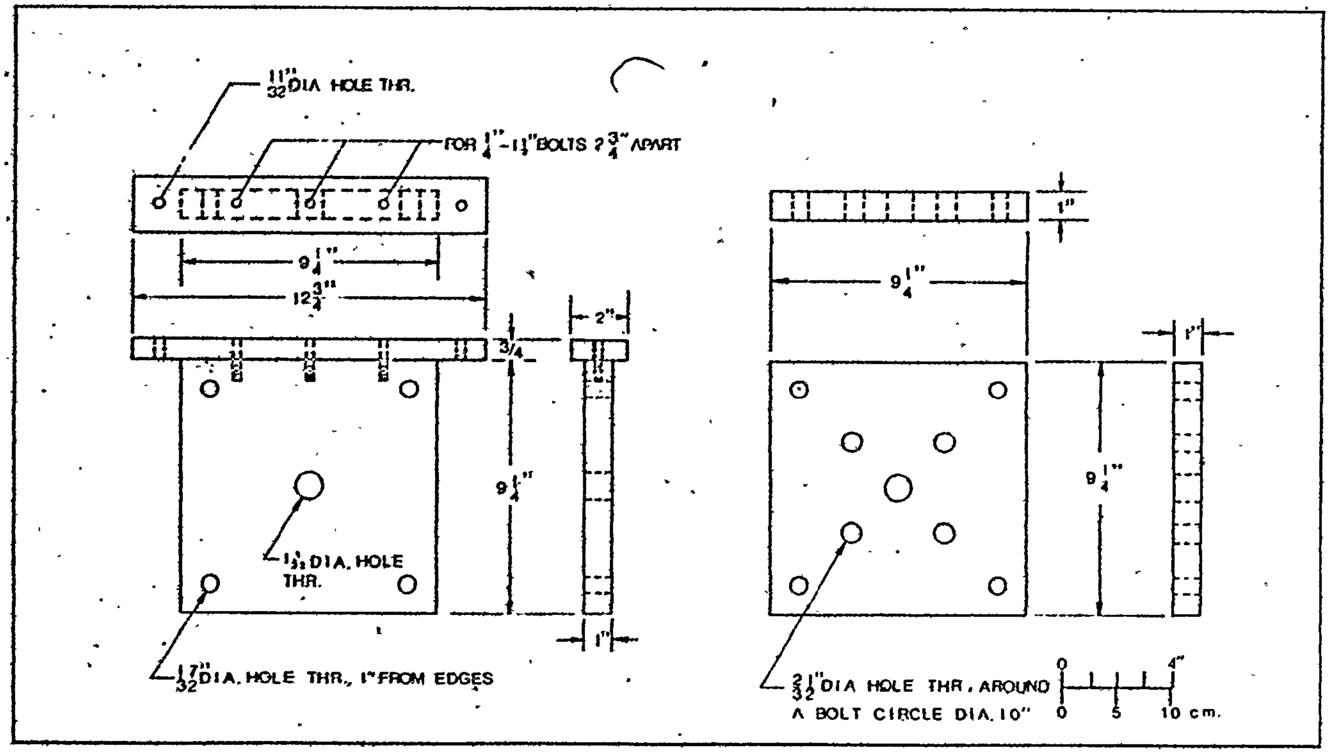

FIGURE 4-13 DESIGN OF TWO STIFF BEARING PLATES OF THE HORIZONTAL LOAD FRAME WITH 20 KN BELLOFRAM ACTUATOR

Moment of inertia of the beam section,

$$I = \frac{1}{12} d^3 \times 107.95 \doteq 9.0 \ d^3 \ mm^4.$$

Stress at the outermost fiber of the beam,

$$f = \frac{Md}{2I} \leqslant 0.61 \ f_y \qquad (4\text{-}4)$$

Substituting the values of M, I and f_y into Equation (4-4) and solving for d gives

$$d = 56.46 \ mm.$$

Based on this calculation, a 57.15 mm ($2\frac{1}{4}$ in.) thick bearing plate was adopted. It should be noted that the beam assumption is conservative since additional strength will be developed in the plate from the other direction. Through a similar approach a 50.80 mm (2 in.) thick plate was selected for the opposite stiff bearing plate, and two 25.40 mm (1 in.) thick plates for the frame containing the Bellofram actuator.

4-10 OTHER PARTS REQUIRED FOR THE CONSTRUCTION OF THE MULTIAXIAL TESTING FRAME

In addition to the stiff bearing plates and tie-rods, some other connecting parts were required for the assembly and the construction of the multiaxial testing frame. These parts included the upper supporting frame, the plates at the back of the actuators to provide attachment to the slings from the upper supporting frame, and parts connected to the actuators and load cells to provide loading caps for the steel balls. Detailed dimensions and drawings of these parts are given in Figures

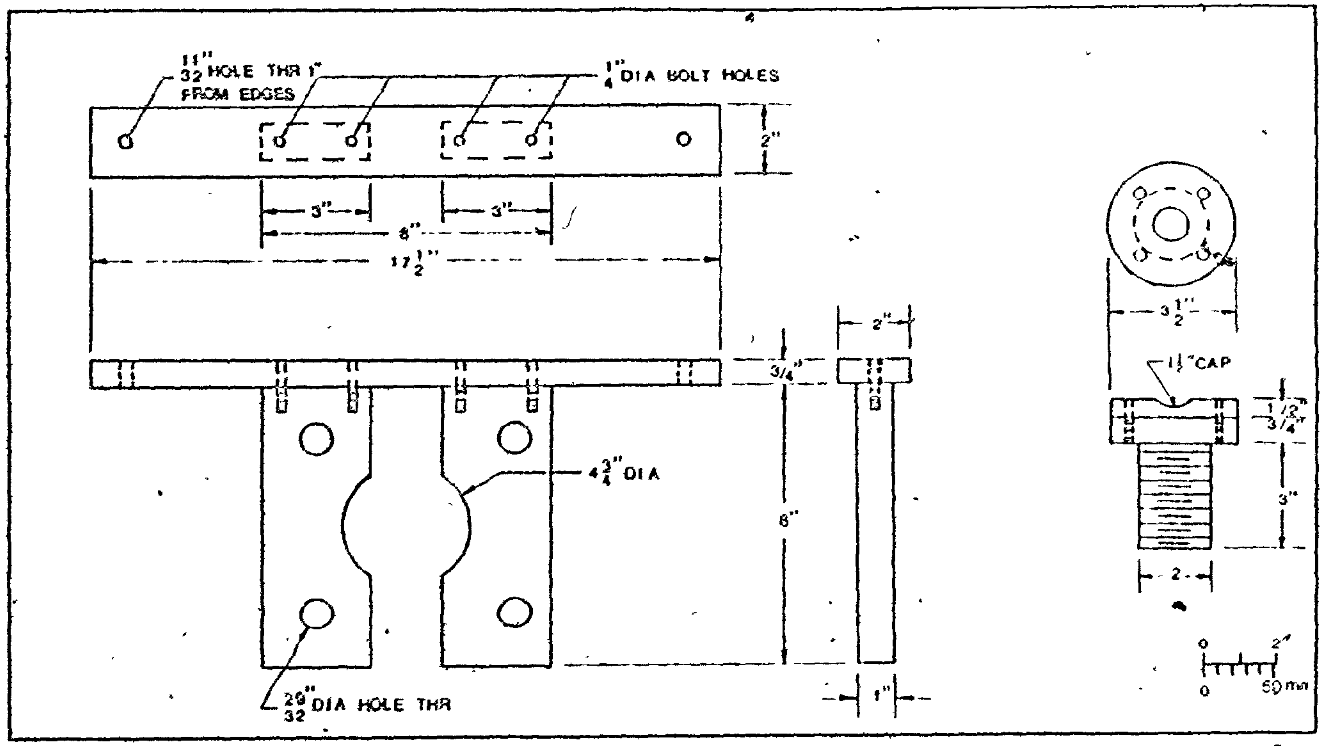

FIGURE 4 -14 CONNECTING PARTS REQUIRED FOR THE CONSTRUCTION OF THE HORIZONTAL LOAD FRAME WITH THE 220 kN MTS ACTUATOR.

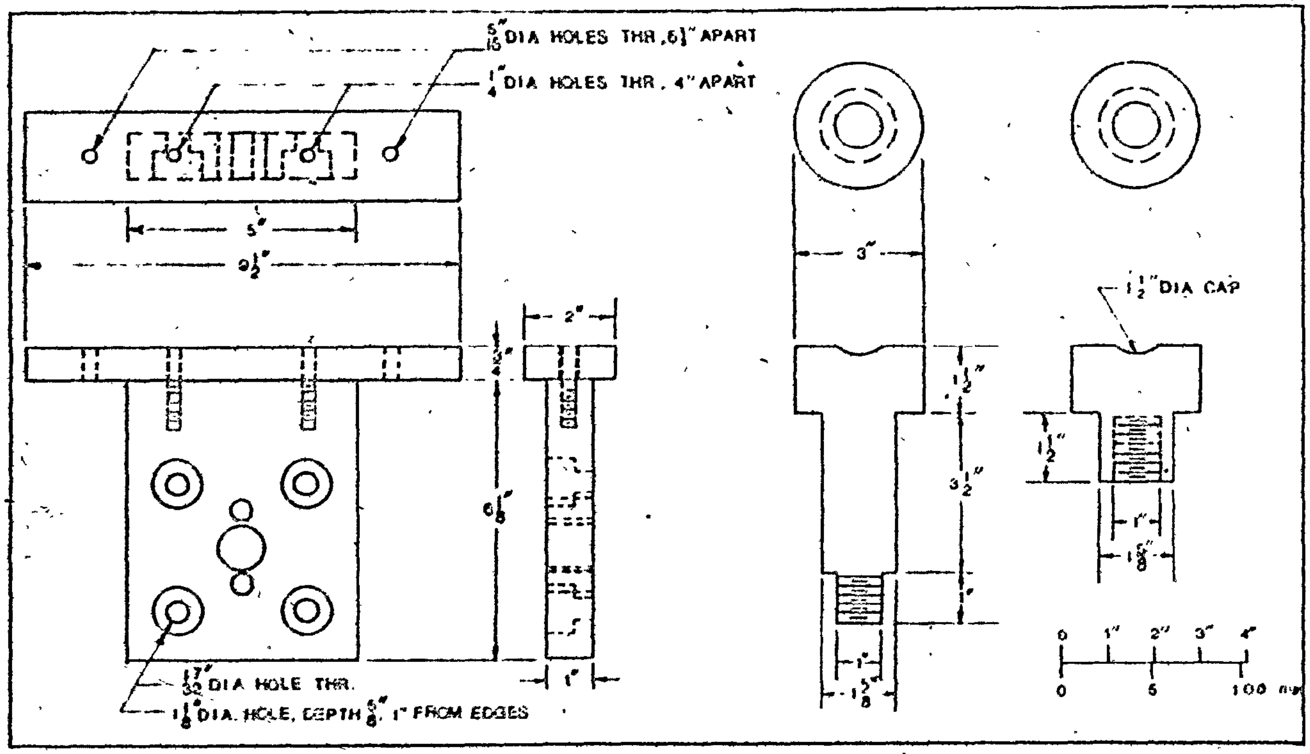

FIGURE 4-15 CONNECTING PARTS REQUIRED FOR THE CONSTRUCTION OF THE HORIZONTAL LOAD FRAME WITH THE 20 KN BELLOFRAM ACTUATOR

4-6, 4-14 and 4-15. The design of these parts satisfied the general design requirements: (1) structually adequate to prevent failure (Factor of safety at least 3), (2) excess deflections and deformations avoided, and (3) dimensions in accord with machining practices.

4-11 ELECTRONIC EQUIPMENT

Most characteristics of the electronic components are temperature dependent. When the electronic equipment is first turned on, the temperature of its components will increase from room temperature to a stable final temperature. The total functional behaviour of the electronic equipment is therefore time-dependent and could introduce errors in the results of creep tests. It is recommended that the characteristics of these circuits be determined in future testing so that the equipment is operating under a stable condition at all times.

CHAPTER 5

CREEP TESTING

5-1 OBJECTIVES

This chapter presents preliminary creep testing data for concrete specimens used to evaluate the multiaxial testing frame. The objectives of these tests were: (1) to examine the performance and limitations of the testing equipment; (2) to develop testing procedures and methods to analyze the resulting experimental data; and, (3) to evaluate some creep characteristics of concrete and compare the results with those available in the literature. Because of the considerable time required for creep tests, the investigation was limited to concrete specimens and only one mix proportion. It was found that the multiaxial frame is capable of simulating different stress states encountered in excavation of tunnels and cuts, and also provided guidelines for rock testing.

5-2 SAMPLE PREPARATION

The creep programme involved 101.6 mm (4 in.) concrete cube specimens with compressive strength characteristic shown in Figure 5-1. The mix proportions, water-cement ratio, curing and properties of the concrete specimens are

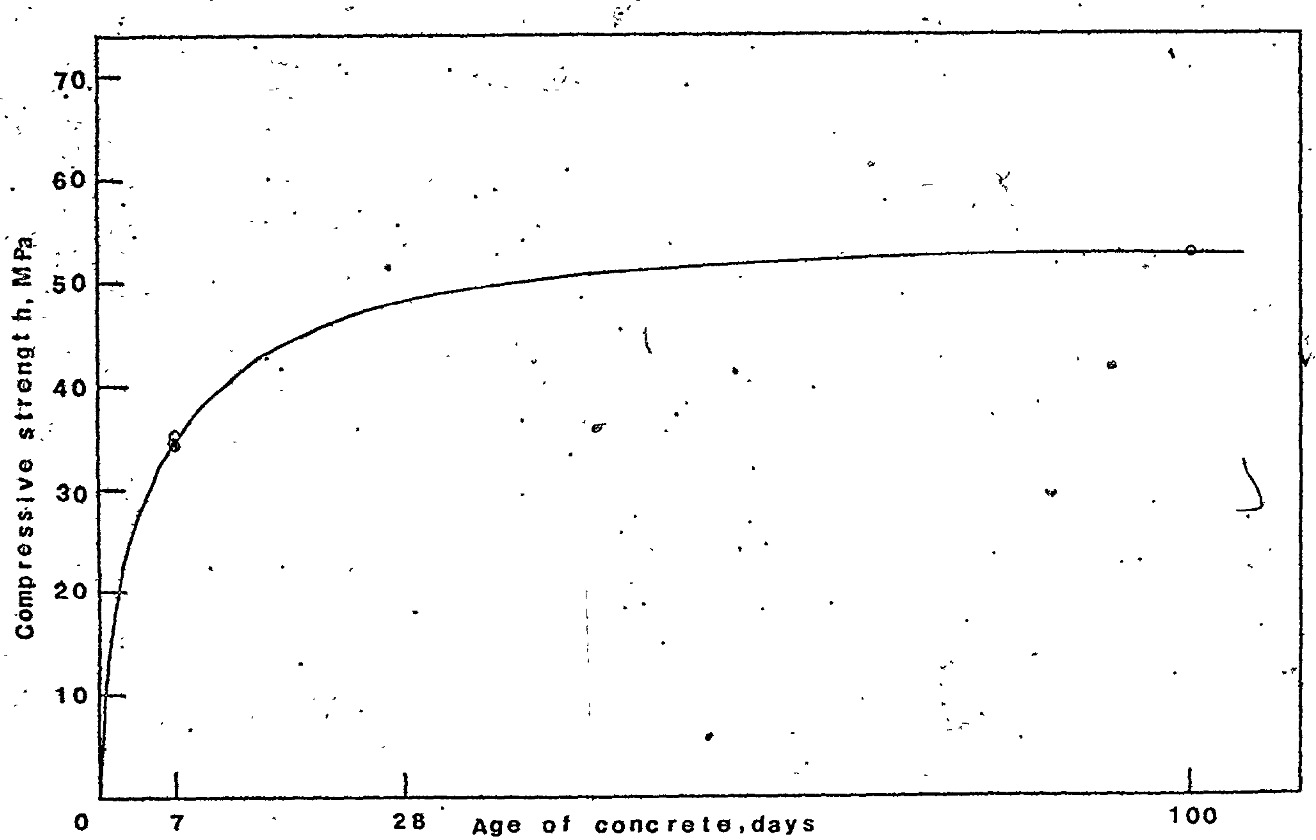

FIGURE 5—1 TEST STRENGTH OF CUBICAL CONCRETE SPECIMENS.

given in Table 5-1. The concrete mix was placed and compacted in plexiglass molds and cured in a wet room until testing.

Although rock creep testing was not included in this programme, two preliminary considerations for the preparation of rock specimens were indicated. The first deals with the case when the bedding is not horizontal as shown in Figure 5-2. Since high lateral stresses depend basically on tectonic history, it is expected that the lateral stresses along the bedding will be practically the same at locations, A, B or C. If a test specimen from the site is prepared such that its edges are parallel and perpendicular to the ground surface, assessment of the lateral stress ratio, K, will be difficult. For this reason, it is recommended that specimens be prepared with their sides parallel and perpendicular to the bedding so that the rock's orthotropic behaviour can still be clearly represented. In this case, the vertical overburden is resolved into two components, σ'_v and τ'_{vh}, perpendicular and parallel to the tangent to the bedding, respectively.

If the angle of dip and the depth are small, and the lateral stresses are large, shear stress influences on rock creep are expected to be insignificant.

Another problem associated with rock sampling is the change in stress state when the rock specimen is brought from the insitu condition to the laboratory. Since rock is a hysteritic material, this release of stress may have some

TABLE 5-1

PROPERTIES OF CONCRETE SPECIMEN

Cement	Ordinary Portland cement
Water-cement ratio	0.39
Mix proportions (by weight) Cement:fine agg.:coarse agg.	1:0.93:1.45
Curing temperature	25°C
Curing relative humidity	98%
Compressive strength	7th day - 34.5 ± 0.6 MPa 100th day - 52.5 MPa

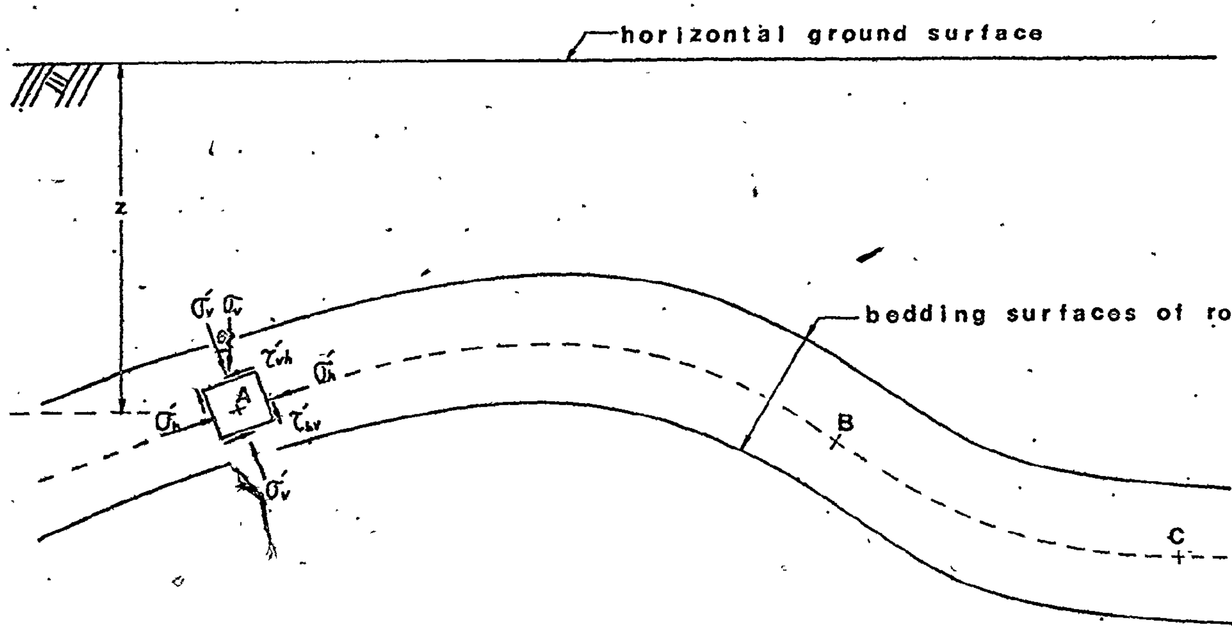

FIGURE 5-2 INITIAL STATE OF STRESS OF A ROCK ELEMENT OF INCLINED ROCK BEDDING.

influence on the monitored creep characteristics of rock. However, if the time between sampling and testing is short, and the rock specimen is brought back to the initial insitu stress state (and environment) with sufficient time to stabilize, the stress change influences are expected to be small. Future testing should include checks on this effect.

5-3 TESTING PROGRAMME

The testing programme, consisting of uniaxial and multiaxial creep tests was designed in such a way as to provide an opportunity to investigate the creep characteristics of concrete as a function of different loading conditions and ages at loading. Owing to the limited time available, most of the creep tests were of less than 4 days duration (i.e. short term tests). Nevertheless, because of the precision of the equipment, the test results were detailed enough to describe the creep characteristics of the specimens even at low strain levels. Most of the specimens were loaded at constant stress for 3 days, when the creep rate was observed to be rather stable, and then followed by a release of loading through the horizontal MTS actuator. This unloading simulates the excavation procedure at sites. Data were collected more frequently at the beginning of load application or the release of stress, since the creep rate is higher at these stages.

5-4 TESTING PROCEDURE

From experience gained in these trial tests, it is recommended that the MTS control unit should be turned on at least four days before any testing is initiated to ensure signal stability. Before any testing, the seating load, the final desired stress levels and the corresponding readings in the load cells, set point dials (indicators on the MTS control unit that control the applied load) and pressure readings should be determined. This procedure is important since it provides enough information during the loading process to eliminate unnecessary time-delays.

Although the laboratory is humidity controlled, a considerable variation of the relative humidity was observed. To eliminate the effect of humidity variations on concrete creep, the specimen was wrapped with a polymer film. During tests, moisture was observed inside the film indicating that humidity changes were mininized. Another purpose of the polymer film was to provide a slip surface between the loading platens and specimen.

After the specimen was wrapped with the polymer film, the next step was application of load. The specimen was inserted into the multiaxial testing frame and a seating load of approximately 16 kN (1.6 MPa) applied in the vertical direction. The specimen was centrally placed so that gaps of similiar size were left on the four sides of the loading platens. This ensures that there will be no direct interaction between two loading platens when the specimen is loaded in the other two directions. Seating loads of approximately 14 kN (1.4 MPa) and 2.5 kN (0.25 MPa) were then applied through the horizontal MTS and Bellofram actuators,respectively. The specimen was then loaded to the desired stress state. While the sequence of loading in the three directions can be arbitary, it is recommended that the vertical load be applied first, so that a more stable condition is reached before applying the horizontal loads. To simulate the process of excavation in these tests, the horizontal actuator was released to the LOW pressure condition (14.3 kN).

5-5 TEST RESULTS

The results of the trial tests are summarized in Table 5-2. A set of typical creep curves for these tests is shown in Figure 5-3. The dashed line represents the creep curve for a uniaxial test (See table 5-2). Data points marked with triangles represent the creep of the specimen along the horizontal MTS actuator, while those marked with circles represent the creep along the vertical MTS actuator. As indicated previously, the monitoring of creep with the Bellofram actuator was not satisfactory. Creep curves for the other tests are given in the Appendix. All the test results show that the creep rates along the two high stress directions (MTS actuators)

TABLE 5-2

SUMMARY OF TESTS

Principal Axes	Loading Actuators	Simulation of Site Conditions	
1	Bellofram	Vertical overburden	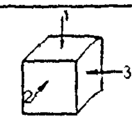
2	Horizontal MTS	Lateral stress, released during excavation	
3	Vertical MTS	Lateral stress	

Test No.	Ages at loading, Temp & R.H.	Axes	Loading conditions (MPa)	$\varepsilon_{el.}$ $(\times 10^{-3})$	$\varepsilon_{c,3\,day}$ $(\times 10^{-6})$	Unloading (MPa)	$\varepsilon_{el.}$ $(\times 10^{-3})$	Squeezing $\varepsilon_{c,1\,day}$ $(\times 10^{-6})$
1	18 days 19.6±0.2°C 66.0±2.7 %		uniaxial 17.0±0.04	11.9	700	--	--	--
2	26 days 19.4±0.25°C 65.8±3.3 %	1 2 3	1.52 17.0±0.024 9.6±0.008	-- 11.6 6.2	-- 630 235	1.52 1.38±0.01 9.60±0.007	-- 10.0 0.12	-- 483 --
3	18 days 19.3±0.3°C 70.0±2.6 %	1 2 3	0.23 17.1±0.013 16.1±0.2	-- 11.2 11.8	-- 570 530	0.23 1.39±0.01 15.8±0.07	-- 9.8 0.19	-- 430 --
4	18 days 19.5±0.4°C 66.0±3.0 %	1 2 3	1.52 17.0±0.016 16.1±0.01	-- 11.1 11.9	-- 560 390	1.52 1.4±0.008 16.1±0.008	-- 9.7 0.14	-- 433 --
5	8 days 19.4±0.25°C 66.3±2.5 %	1 2 3	1.52 17.0±0.02 16.1±0.008	-- 11.4 12.0	-- 780 640	1.52 1.37±0.01 16.1±0.004	-- 9.9 0.18	-- 490 --
6	12 days 19.5°C 66.3±0.6 %	1 2 3	1.52 17.0±0.004 16.1±0.008	-- 11.7 12.0	-- -- --	-- -- --	-- -- --	-- -- --
7	160 days 19.5°C 69.2±2.6 %	1 2 3	1.52 17.0±0.013 16.1±0.03	-- 11.1 --	-- 520 440	1.52 1.38±0.015 16.1±0.007	-- 9.7 0.084	-- 420 --

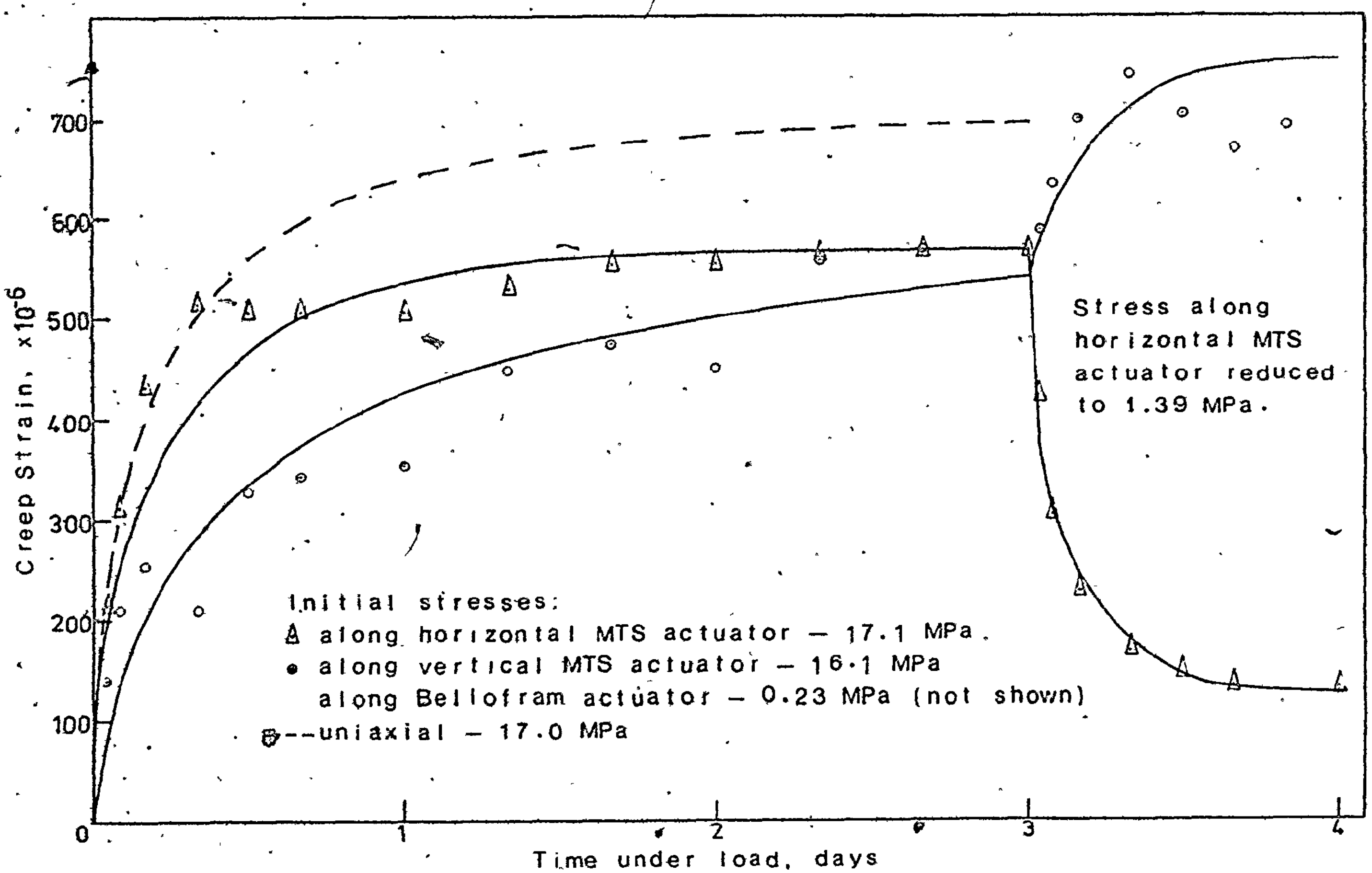

FIGURE 5-3 CREEP CURVES; TEST NO.1 AND 3 - 18 DAYS OF CURING.

are quite fast right after loading and the primary creep stage is essentially completed in one day. The creep rates became rather stable after the second day, and creep was essentially complete after three days. After the release of loading through the horizontal MTS actuator, the specimen rapidly "squeezes" in this direction and further creep is observed in the other direction, as indicated by the two curves in the figure. The creep rates drop rapidly and creep was essentially complete after one day. An average ratio of one-day creep strain after unloading to three-day creep strain under loading for the same specimens was found to be 0.75, strongly indicating the squeezing effect due to unloading conditions.

The creep and squeezing behaviour of the concrete specimen is characterized by a short primary creep stage and a low-rate secondary creep stage. Reasons for this observed behaviour are: (1) the water-cement ratio of the concrete specimen is low (0.39); (2) the stress-strength ratio (approximately from 0.4 to 0.5) is low; and (3) the specimen is wrapped with polymer film. In fact, a much longer primary creep stage was observed for the concrete specimen loaded after 8 days curing since the stress-strength ratio was higher.

The creep and squeezing behaviour of the concrete specimens for all tests are compared in Figures 5-4 to 5-7. Curves and data points in Figures 5-4 and 5-5 represent creep and squeezing of specimens after different curing times, respectively. Both cases show that creep and squeezing decreases with concrete

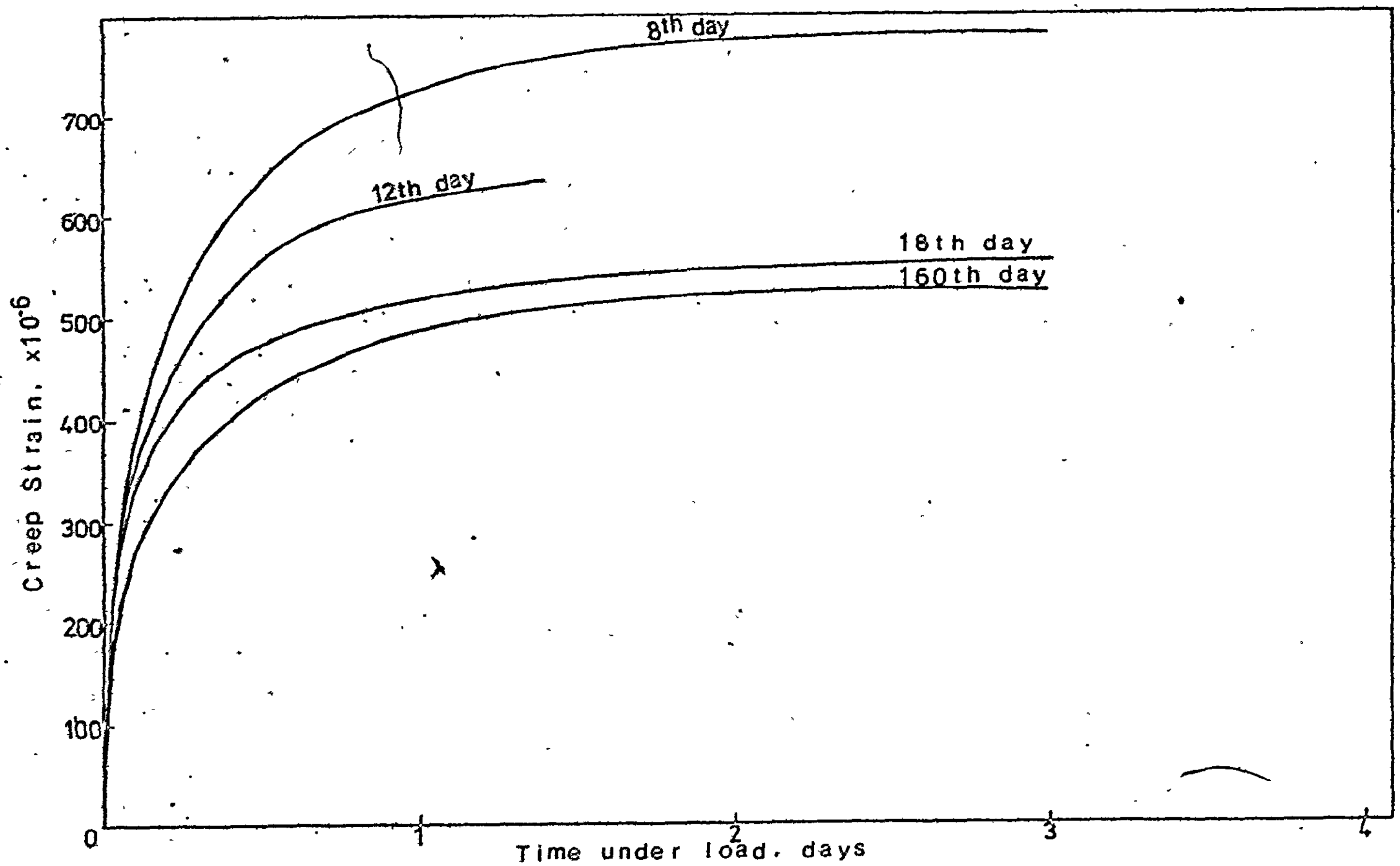

FIGURE 5-4 CREEP OF SPECIMENS ALONG THE DIRECTION OF HORIZONTAL MTS ACTUATOR; WITH DIFFERENT AGES AT LOADING.

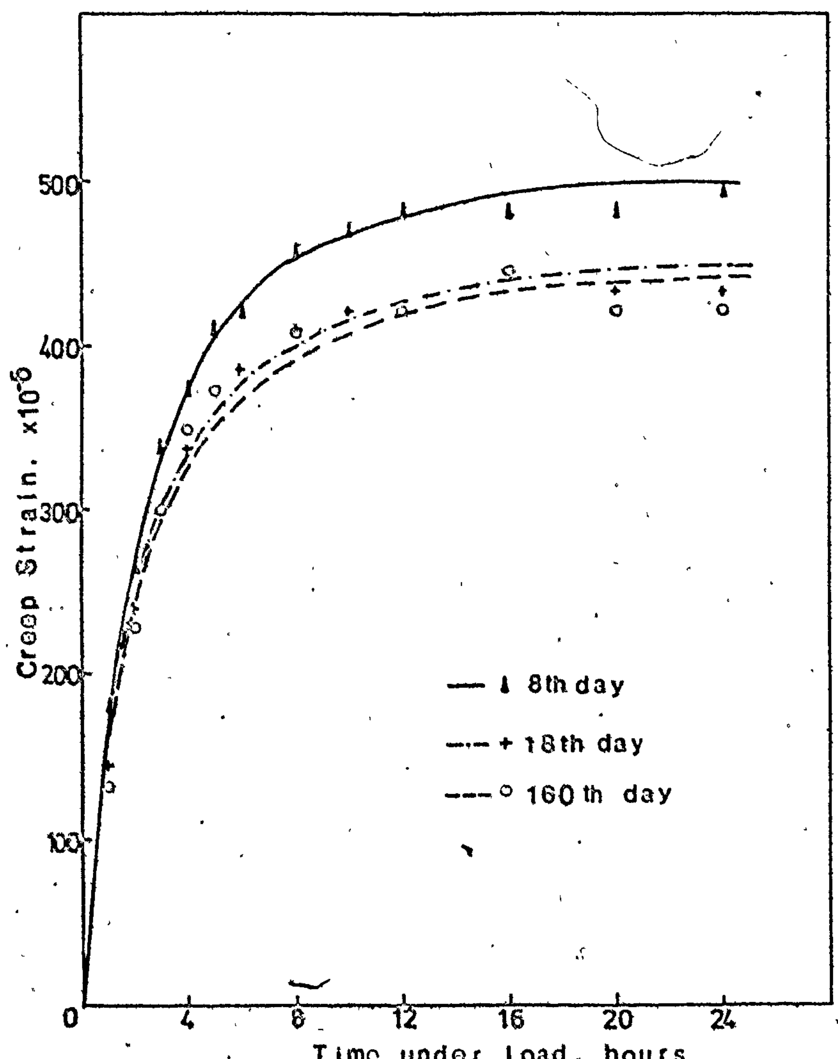

FIGURE 5-5 SQEEZING OF SPECIMENS WITH DIFFERENT AGES AT LOADING UPON UNLOADING OF THE HORIZONTAL MTS ACTUATOR.

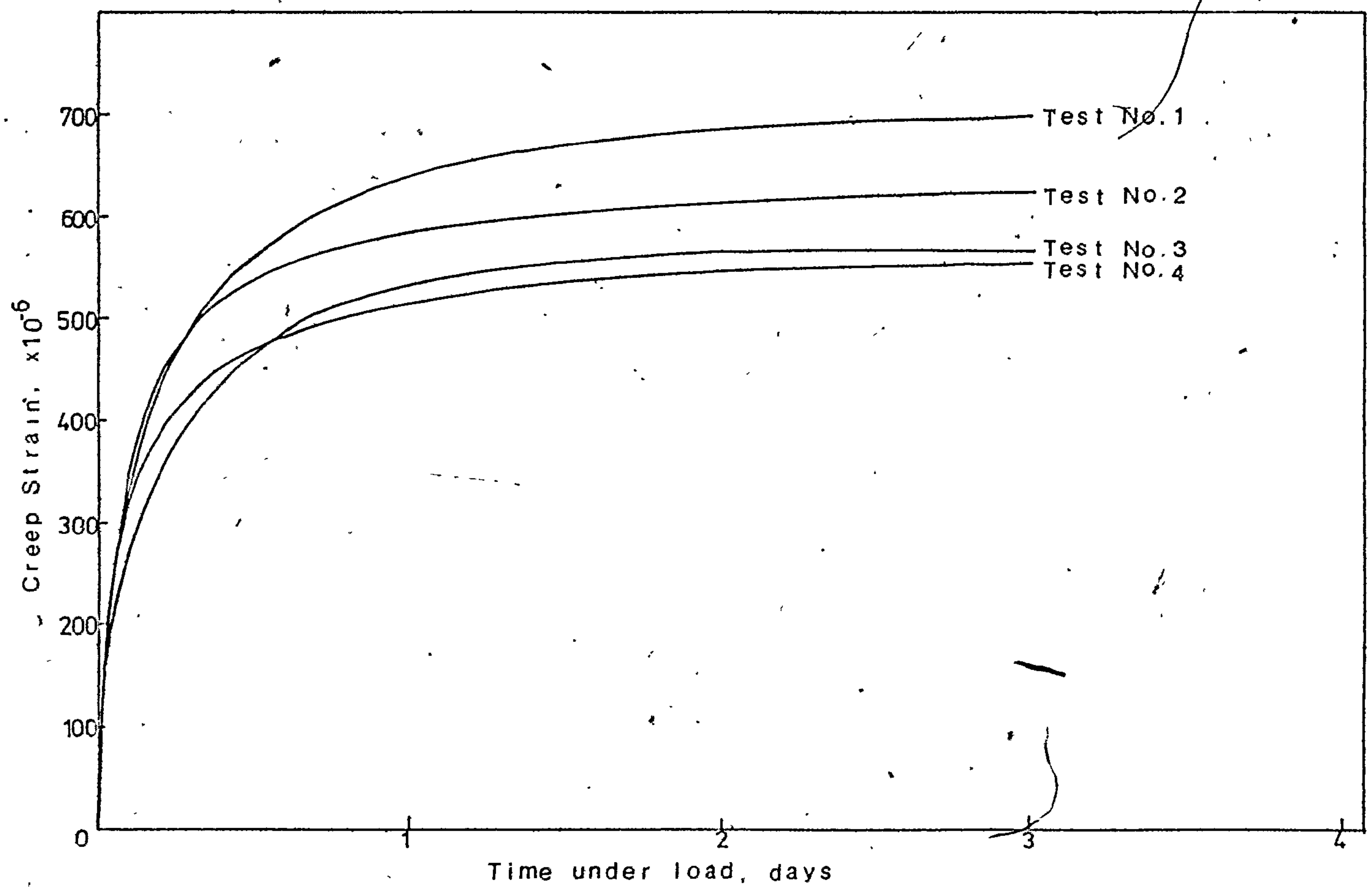

FIGURE 5-6 CREEP OF SPECIMENS ALONG THE DIRECTION OF THE HORIZONTAL MTS ACTUATOR; UNDER DIFFERENT LOADING CONDITIONS.

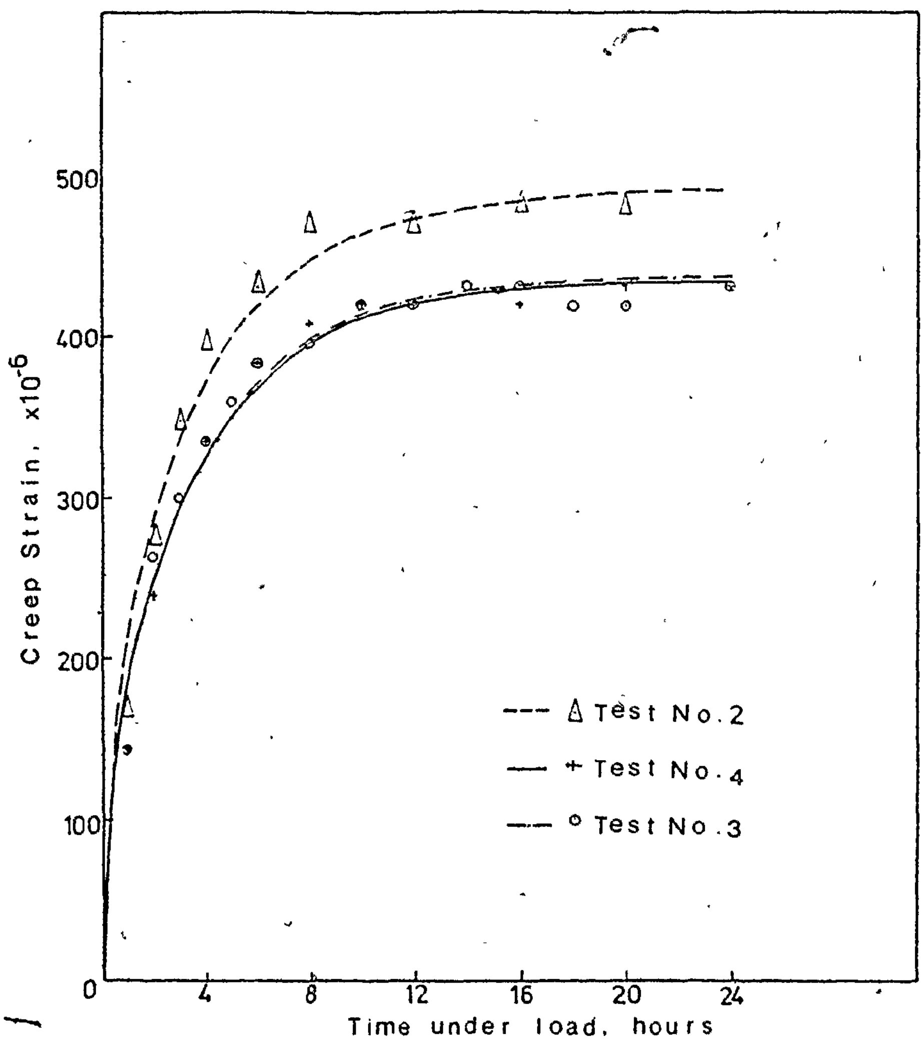

FIGURE 5-7 SQEEZING OF SPECIMENS LOADED WITH DIFFERENT CONDITIONS UPON THE UNLOADING OF THE HORIZONTAL MTS ACTUATOR.

maturity, as anticipated. Figure 5-6 shows the creep of specimens along the horizontal MTS actuator direction under four different loading conditions. Creep in this direction was observed to decrease with increased loading in the other two directions. Figure 5-7 shows the squeezing of specimens which were loaded with three different loading conditions for three days, followed by the release of the loading along the horizontal MTS actuator direction. No significant difference was observed between test 3 and 4 in which the stresses along the Bellofram actuator are 0.23 and 1.52 MPa repectively. This may be due to the small difference between the two stress levels along this direction. It was also noted that the squeezing was greater in test 2, in which the stress level along the vertical MTS actuator direction is lower. This is as expected since the confining stress is smaller. However, the validity of this test result requires further experimental support.

5-6 LIMITATIONS

The stress levels generated by the three actuators of the multiaxial testing frame are limited to approximately 17 MPa and 1.5 MPa for the two MTS actuators and the Bellofram actuator, repectively. This capacity of the Bellofram actuator limits tunnel excavation simulation to depths less than 70 m. Since the deformation of specimens along this direction cannot be obtained without further LVDT development, the use of Equation (2-7) to verify the test results is impossible at this time.

CHAPTER 6

CONCLUSION AND RECOMMENDATION

6-1 CONCLUSION

Although the multiaxial creep testing frame developed has limitations requiring further study, typical stress paths involved during rock excavation were simulated with concrete specimens and continuous monitoring of loads and displacements. Limited experimental results from the trial testing programme showed some agreement with theory. However, significant further testing is required for validations and/or development of creep relationships. The generalization of uniaxial creep relationships to the multiaxial case was not possible since the creep strain in one of the principal directions was not determined. However, the testing programme provided recommendations to overcome this limitation.

6-2 RECOMMENDATIONS

The creep behaviour of rock and concrete depends on temperature and humidity. It is therefore very important to maintain a test environment similiar to insitu conditions. It is recommended that a chamber be used to surround the specimen so that the temperature and humidity can be adjusted to any desired levels.

MTS actuator of higher capacity is recommended to take the place of the Bellofram actuator so that rock at greater depths can be represented. The replacement of the Bellofram with an MTS actuator will also enable the measurement of specimen strain in this direction, so that enough information will be available to generalize typical uniaxial creep relationships to the multiaxial insitu condition.

REFERENCES

1. Afrouz, A. and Harvey, J.M., "Rheology of rocks within the soft to medium strength range", International Journal of Rock Mechanics and Mining Sciences, Volume 11, 1974, Page 281-290.

2. Boresi, A.P. and Deere, D.U., Creep Closure of a Spherical Cavity in an Infinite Medium, Holmes Narver Incorporated, Las Vegas, 1963.

3. Cogan, J., "Triaxial Creep Tests of Opohonga Limestone and Ophir Shale", International Journal of Rock Mechanics and Mining Sciences and Geomechanics Abstract, Pergamon Press, Volume 13, 1976, Page 1-10.

4. Cridland, L., Bakoss, S.L. and Burfitt, A.J., "A Low-cost creep rig for concrete", Magazine of Concrete Research, Volume 29, Number 100, 1977, Page 147-150.

5. Desai, C.S., "Overview, trends and projections: theory and applications of the finite element method in geotechnical engineering, state-of-the-art", In: Desai, C.S. (Editor), Applications of the Finite Element Method in Geotechnical Engineering, Corps of Engineers, Vicksburg, Massachusetts, Volume 1, 1972, Page 3-90.

6. Desai, C.S. and Abel, J.F., Introduction to the Finite Element Method, A Numerical Method for Engineering Analysis, Van Nostrand Reinhold, New York, 1972.

7. Deane, L. (Editor), Instruction Manual, Model PD-2064, Key Programmable Data Acquisition System, Third Printing, Angus Instrument Coporation, Indianapolis, Indiana, 1975.

8. Design Manual, Bellofram, Bellofram Corporation, Burlington, Massachusetts, 1962.

9. Dorn, J.E. et al, "Plastic Flow in Metals", War Production Report, Number 200, 1945 (Given in: Lubahn I.D. and Felgar, R.P., Plasticity and Creep of Metal, Wiley, New York, 1961).

10. Duncan, N., Engineering Geology and Rock Mechanics, Volume I and II, International Textbook, England, 1969.

11. Emery, J.J., Finite Element Analysis of Creep Problems in Soil Mechanics", Doctor of Philosophy Thesis, University of British Columbia, 1971.

12. Emery, J.J., "Simulation of slope creep", In: Voight B. (Editor), Developments in Geotechnical Engineering 14A, Rockslides and Avalanches, 1, Natural Phenomena, Elsevier Scientific Publishing Company, New York, 1978, Chapter 19, Page 669-691.

13. Emery, J.J., Hanafy, E.A. and Franklin, J.A., "Creep movements associated with excavations in rock", In: Geddes (Editor), Large Ground Movements and Structures, Proceedings of the Conference held at the University of Wales, Institute of Science and Technology, Cardiff, 1977, Pentech Press, London, 1977, Page 387-410.

14. Farmer, I.W., Engineering Properties of Rocks, 1971, Spon, London, 1968.

15. Franklin Trow Associates Limited, Personal Communication, Rexdale, 1975.

16. Goodman et al., "A model for the Mechanics of Jointed Rock", Journal of the Soil Mechanics and Foundation Division, American Society for Civil Engineers, Number SM 3, Volume 94, 1968, Page 637-659.

17. Gopalakrishnan, K.S., Neville, D.M. and Ghali, A., "Creep poisson's ratio of concrete under multiaxial compression", Journal of the American Concrete Institute, Title number 66-90, 1969, Page 1008-1019.

18. Green, G.E., "Strength and Deformation of Sand measured in an Independent Stress Control Cell", In: Parry, R.H.G. (Editor), Stress Strain Behaviour of Soils, Proceedings of the Roscoe Memorial Symposium, Cambridge University, March, 1971, Foulis Company, Oxfordshire, Britain, 1972, Page 285-323.

19. Hanafy, E.A., "Finite Element Simulation of Tunnel Excavation in Creeping Rock", Master of Engineering Thesis, McMaster University, Hamilton, 1976.

20. Hanafy, E.A. and Emery, J.J., "Advancing face simulation of tunnel excavations and lining placement", Underground rock engineering, 13th Canadian Rock Mechanics Symposium, Toronto, May, 1980, The Canadian Institute of Mining and Metallurgy, Special Volume 22, Page 119-125.

21. Hirst, T.J. and Mitchell, J.K., "Compositional and environmental influences on the stress-strain-time behaviour of soils", Rep., Number TE-68-4, Department of Civil Engineering, University of Californaia, Berkeley, 1968.

22. Hobbs, D.W., "Stress-strain-time behaviour of a number of Coal measure rocks", International Journal of Rock Mechanics and Mining Sciences, Volume 7, 1970, Page 149-170.

23. Hobbs, D.W., Technical Report, Strength and Deformation Properties of Plain Concrete subject to Combined Stress, Part 2: Strength in Multiaxial Compression, Cement and Concrete Association, London, March, 1972.

24. Illston, J.M., "Creep of Concrete", In: Pomeroy, C.D. (Editor), Creep of Engineering Materials, Mechanical Engineering Publications Limited, London, 1978, Page 47-65.

25. Illston, J.M. and Jordaan, I.J., "Creep prediction of concrete under multiaxial stress", Journal of the American Concrete Institute, Volume 69, Title Number 69-14, 1972, Page 158-164.

26. Instruction Manual, MTS Ref. 809.09, Materials Testing System Division, Research Incoporated, Minneapolis, Minnesota.

27. International Critical Tables, 1927.

28. Jaeger, C., Rock Mechanics and Engineering, Cambridge University Press, London, 1972.

29. Jordaan, I.J. and Illston, J.M., "Time-dependent strains in sealed concrete under systems of variable multiaxial stress", Magazine of Concrete, Concrete Research, Volume 23, Number 75-76, 1971, Page 79-88.

30. Karapetian, K.S., "Influence of anisotropy of concrete on creep in compression and tension as a function of size of specimen", Akad. Nauk Armianskoi SSR, Fiziko-Mathematicheskie-Estestvennye 17, Number 4, 1964.

31. Kessler and Sligh, Research Paper, RP 1320, U.S. Bureau of Standards, 1940.

32. Kondner, R.L. and Krizek, R.J., "Creep compliance response of a cohesive soil", Journal of Franklin Institute, 279(5), 1965, Page 366-373.

33. Kolsovos, M.D. and Newman, J.B., "A mathematical description of the deformational behaviour of concrete under complex loading", Magazine of Concrete Research, Volume 31, Number 107, 1979, Page 77-90.

34. Krishnaswamy, K.T., "Strength and microcracking of plain concrete under triaxial compression", Journal of the American Concrete Institute, Proc. 65, 1968, Page 856-862.

35. Kulhawy, F.H., "Finite element modelling criteria for underground openings in rock", International Journal of Rock Mechanics and Mining Sciences, Volume 11, 1974.

36. Lane, K.S., "Field test sections save cost in tunnel support", Report from Underground Construction Research Council, American Society of Civil Engineers, New York, 1975.

37. Lliboutry, L., "Traite de Glaciologie", Tome II, Masson, Paris, 1965, Page 640-652.

38. Meek, J.L., "Excavation in Rock; an application of the finite element method of analysis", Proceedings of the 1973 Tokyo Seminar on Finite Elemnet Analysis, University of Tokyo Press, Tokyo, 1973.

39. Meier, M.F., "Mode of flow of Saskatchewan Glacier, Alberta, Canada", Professional Paper, U. S. Geological Survey, Number 351, 1960.

40. Mills, L. and Zimmerman R., "Compressive strength of plain concrete under multiaxial loading conditions", Journal of the American Concrete Institute, Proceedings 67, Page 802.

41. Mitchell, J.K., Campanella, R.G. and Singh, A., "Soil creep as a rate process", Proceedings of the American Society of Civil Engineers, Journal of Soil Mechanics and Foundation Division, Number SM 1, Volume 94, 1968, Pages 231-254.

42. Morton, J.D., Lo, K.Y. and Belshaw, D.J., " Rock performance considerations for shallow tunnels in bedded shales with high lateral stresses", Proceedings of the 12th Canadian Rock Mechanics Symposium, Queen's University, Kingston, 1975.

43. Neville, A.M., Creep of Concrete: Plain, Reinforced and Prestressed, North-Holland, Amsterdam, 1970.

44. Nguyen, T.Q., "Simulation of ice flow using the finite element method, Master of Engineering Thesis, McMaster University, Hamilton, 1976.

45. Nye, J.F., "The flow of ice from measurements in Glacier Tunnels, Laboratory experiments and the Jungfranfirn Borehole experiment", Proceedings of Royal Society, Series A, Volume 219, Number 1139, 1953, Page 477-489.

46. Operator's Manual, Model 901.77, Material Testing System Division, Research Incoporated, Minneapolis, Minnesota, 1966.

47. Pauw, A., "Static Modulus of Elasticity of Concrete as affected by density", Journal of the American Concrete Institute, Proceedings 57, December, 1960.

48. Palmer, J.H.L. and Lo, K.Y., "Insitu stress measurements in some nearsurface rock formation - Thorold, Ontario", Porceedings of the 28th Canadian Geotechnical Conference, Canadian Geotechnical Society, Montreal, 1975.

49. Peng, S.S., "Time-dependent aspects of rock behaviour as measured by a servocontrolled hydraulic testing machine", International Journal of Rock Mechanics and Mining Sciences and Geomechanics Abstract, Volume 10, Pergamon Press, 1973, Pages 235-246.

50. Pomeroy, C.D., "Time-dependent deformation of rocks", In: Pomeroy, C.D. (Editor), Creep of Engineering Materials, Mechanical Engineering Publication Limited, London, 1978, Page 1-10.

51. Radhakrishnan, N. and Reese, L.C., "A review of applications of the finite element method of analysis to problems in soils and rock mechanics", Soils and Foundations, Volume 10, Number 3, 1970, Page 95-112.

52. Reik, G. and Zacas, M., "Strength and deformation characteristics of jointed media in true triaxial compression", International Journal of Rock Mechanics and Mining Sciences and Geomechanics Abstract, Volume 15, 1978, Pergamon Press, Page 295-303.

53. Robertson, E.C., "Viscoelasticity of rocks", Proceedings of the International Conference on the State of Stress in the Earth's Crust, Elsevier, Santa Monica, 1963.

54. Scott, R.F. and Ko, H., "Stress-deformation and strength characteristics", 7th International Conference on Soil Mechanics and Foundation Engineering, State of the Art Volume, 1969, Page 1-47.

55. Schiffman, R.L., "The use of viscoelastic stress-strain laws in soil testing", American Society for Testing Materials, Special Technical Publication, Volume 254, 1959, Page 131-155.

56. Shank, J.R., "The plastic flow of concrete", Bulletin Number 91, Ohio State University Engineering Experiment Station, 1935.

57. Shank, J.R., "The Mechanics of Plastic Flow of Concrete", Proceedings of the American Concrete Institute, Volume 32, 1936.

58. Singh, D.P., "A study of creep of rocks", International Journal of Rock Mechanics and Mining Sciences and Geomechanics Abstract, Pergamon Press, Volume 12, 1975, Page 271-276.

59. Spooner, D.C., "Stress-strain-time relationships for concrete", Magazine of Concrete Research, Volume 23, Number 75-76, 1971, Page 127-131.

60. Straub, L.G., "Plastic flow in concrete arches", Journal of the Structural Division, American Society for Civil Engineers, Volume 56, 1930, Page 49-114.

61. Valsangkar, A.J. and Gokhale, K.V.G.K., "Stress-strain relationships for empirical equations of creep in rocks", Engineering Geology, Elsevier Publishing Company, Amsterdam, 1972, Page 49-53.

62. Williams, F.T. and Elizzi, M.A., "Technical Note: An Apparatus for the Determination of time dependent behaviour of Rock under Triaxial Loading", International Journal of Rock Mechanics and Mining Sciences and Geomechanics Abstract, Pergamon Press, Volume 13, 1976, Page 245-248.

63. Yuen, C.M.K., Lo, K.Y. and Leonards G.A., " A new apparatus for measuring the principal strains in anisotropic clays", Geotechnical Testing Journal, Volume 1, Number 1, March 1978, Page 24-33.

64. Zienkiewicz, O.C., The Finite Element Method, the third edition, McGraw Hill Book Company, (UK) Limited, London, 1977.

65. Zienkiewicz, O.C., "Continiuum mechanics as an approach to rock mass problems", In: Stagg, K.G. and Zienkiewicz, O.C., (Editors), Rock Mechanics in Engineering Practice, Wiley, London, 1968.

APPENDIX

SUPPLEMENTARY FIGURES

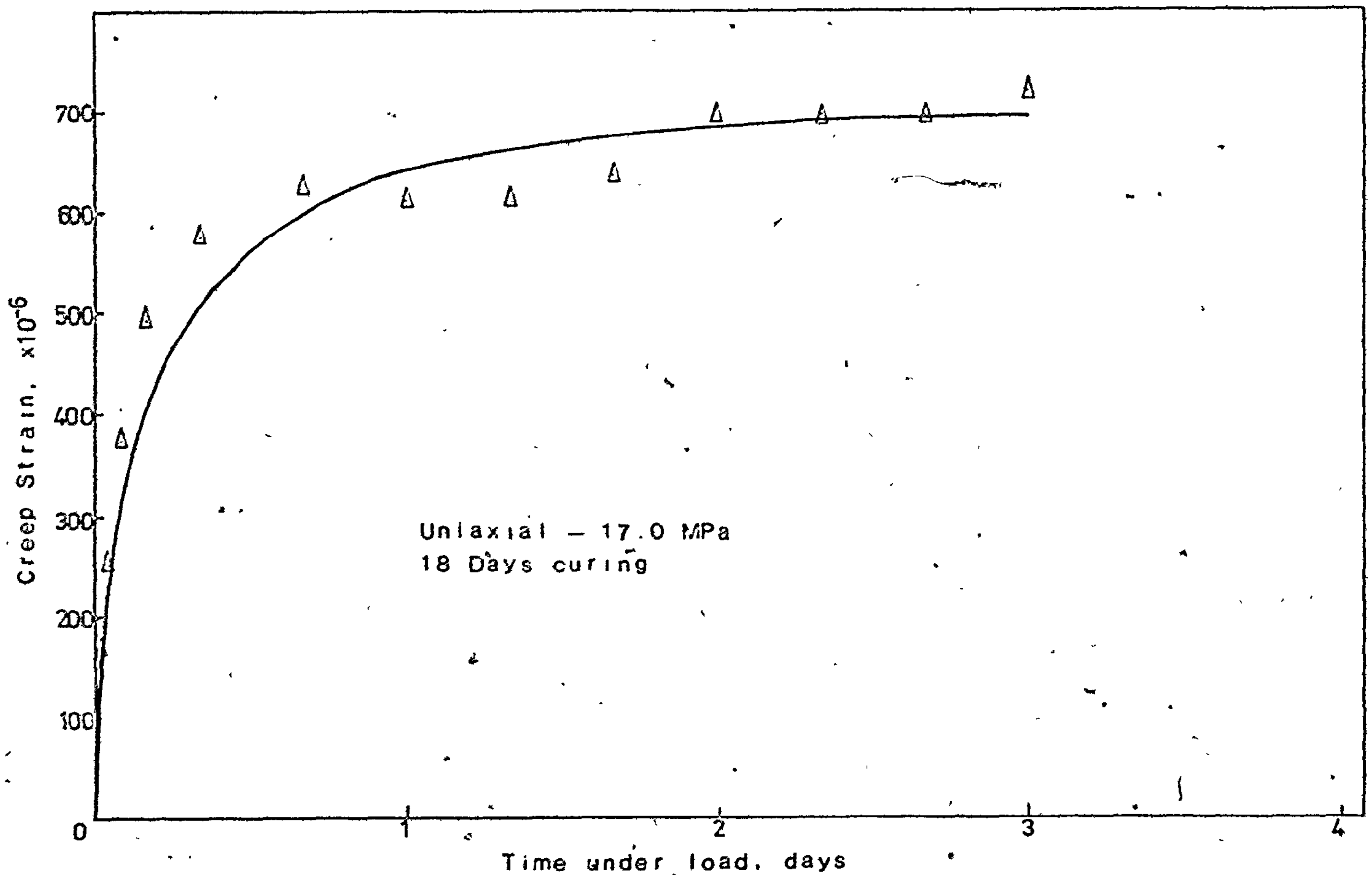

FIGURE A-1 CREEP CURVE: TEST NO.1.

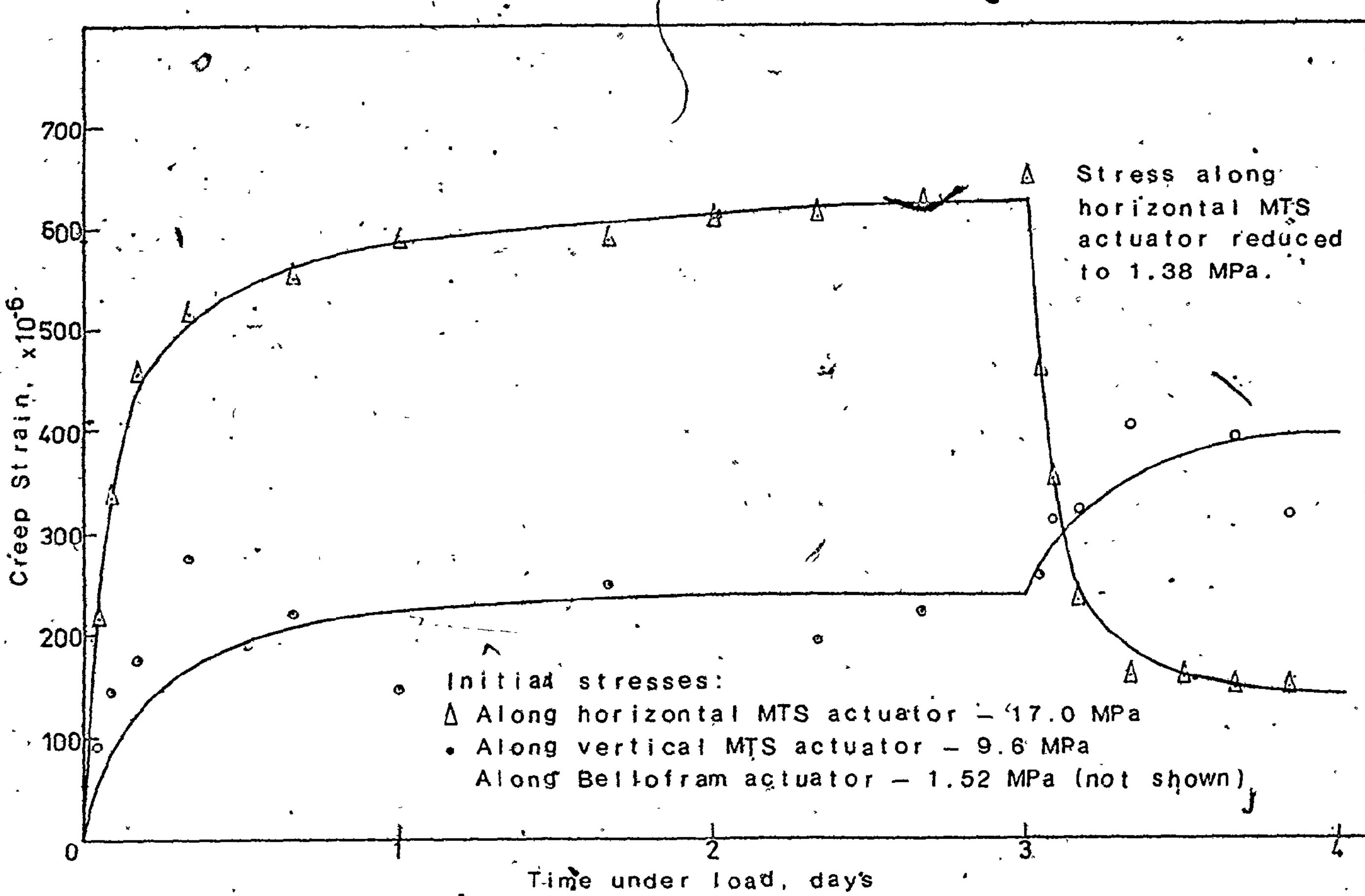

FIGURE A-2 CREEP CURVES: TEST NO.2 – 26 DAYS CURING.

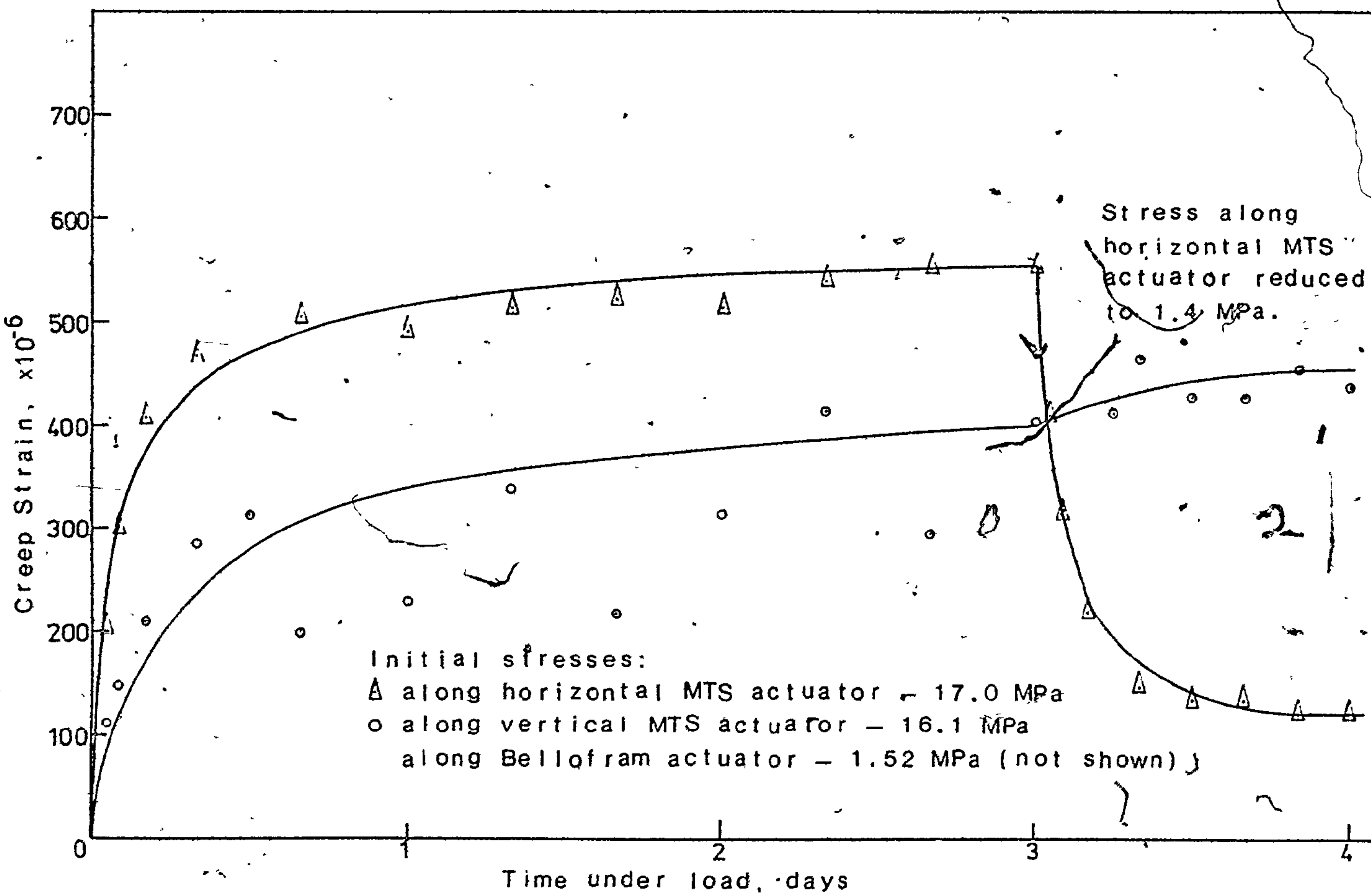

FIGURE A-3 CREEP CURVES: TEST NO. 4 – 18 DAYS CURING.

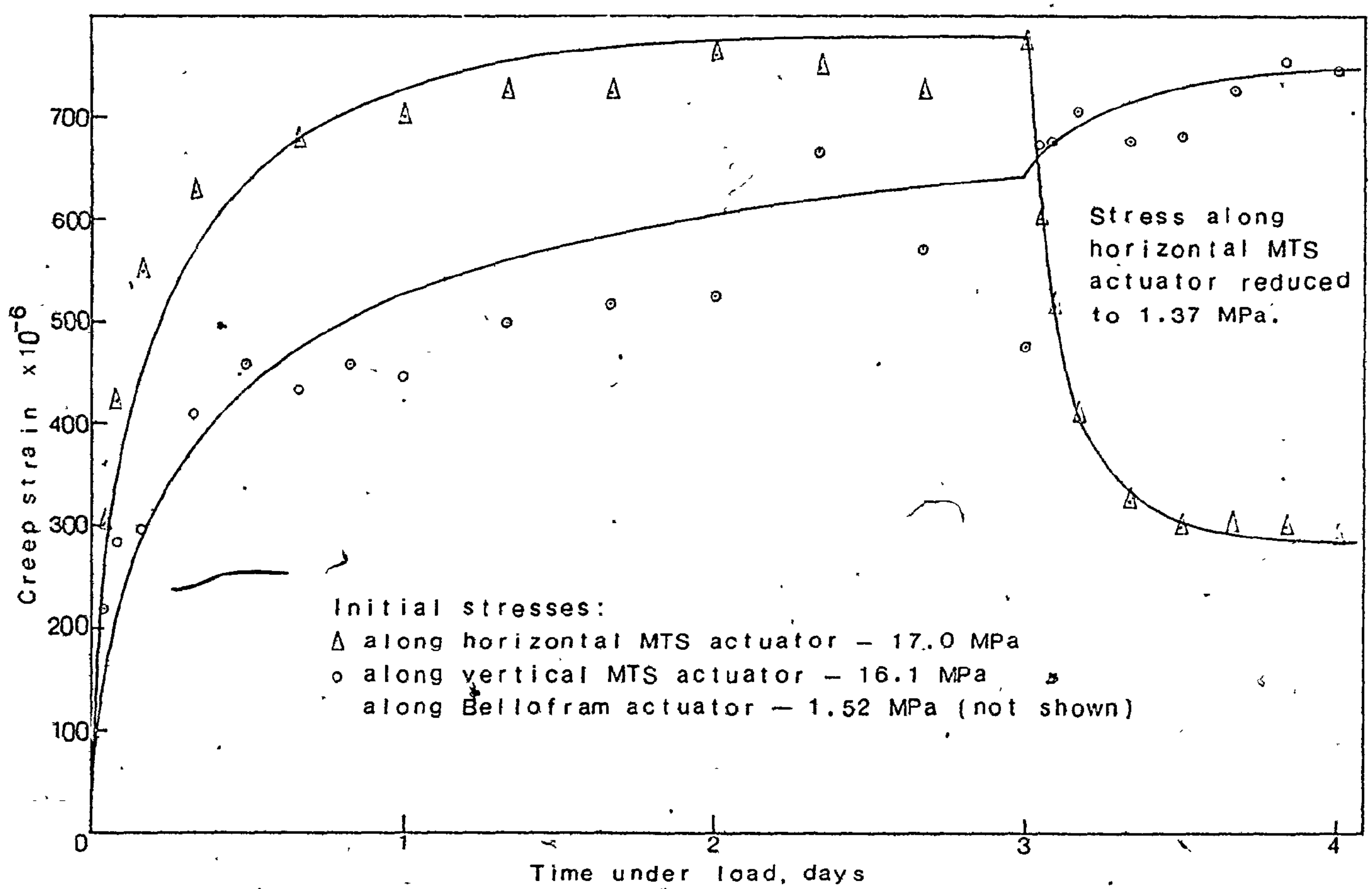

FIGURE A-4 CREEP CURVES; TEST NO.5 — 8 DAYS CURING.

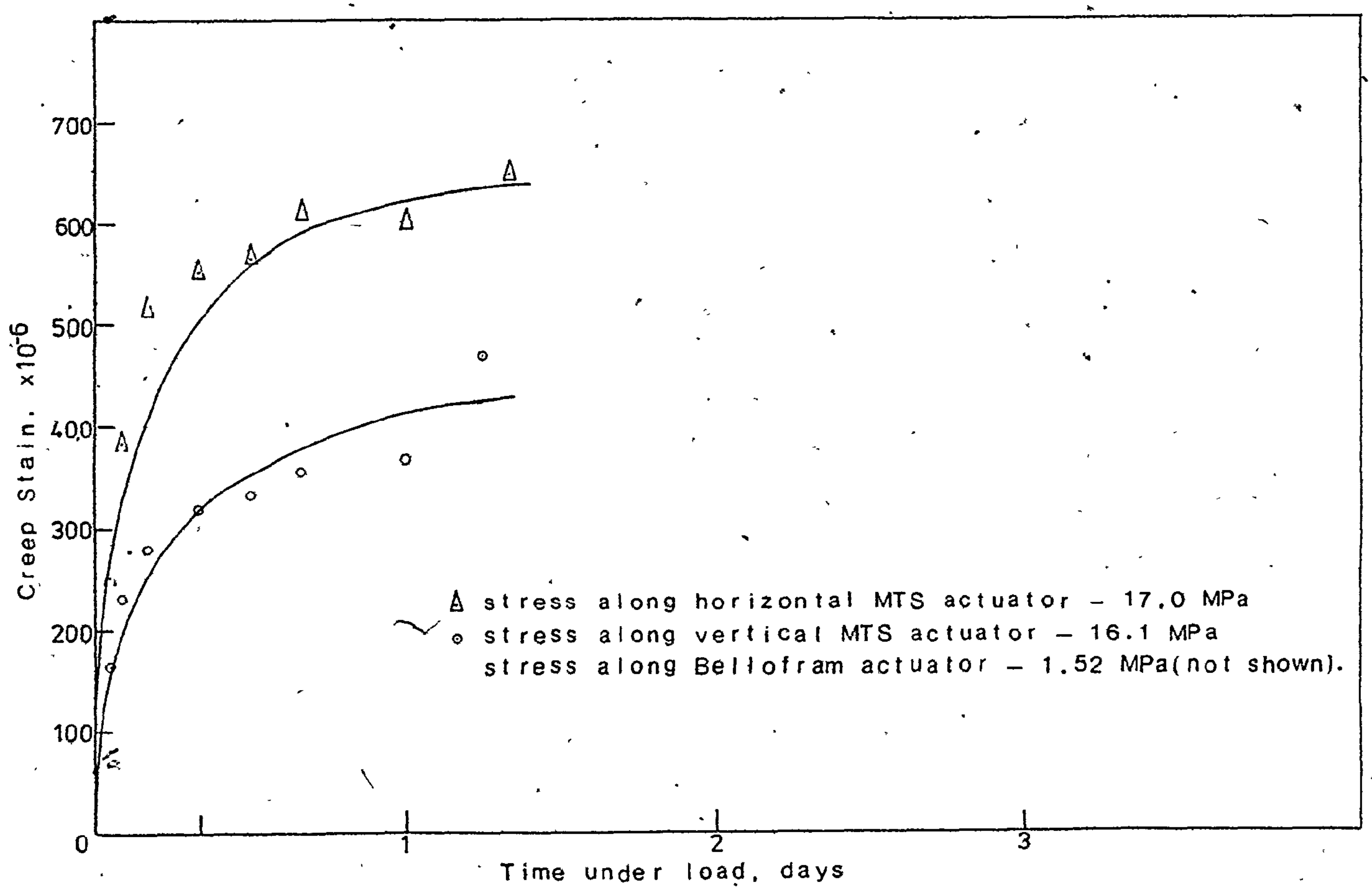

FIGURE A-5 CREEP CURVES: TEST NO.6 — 12 DAYS CURING.

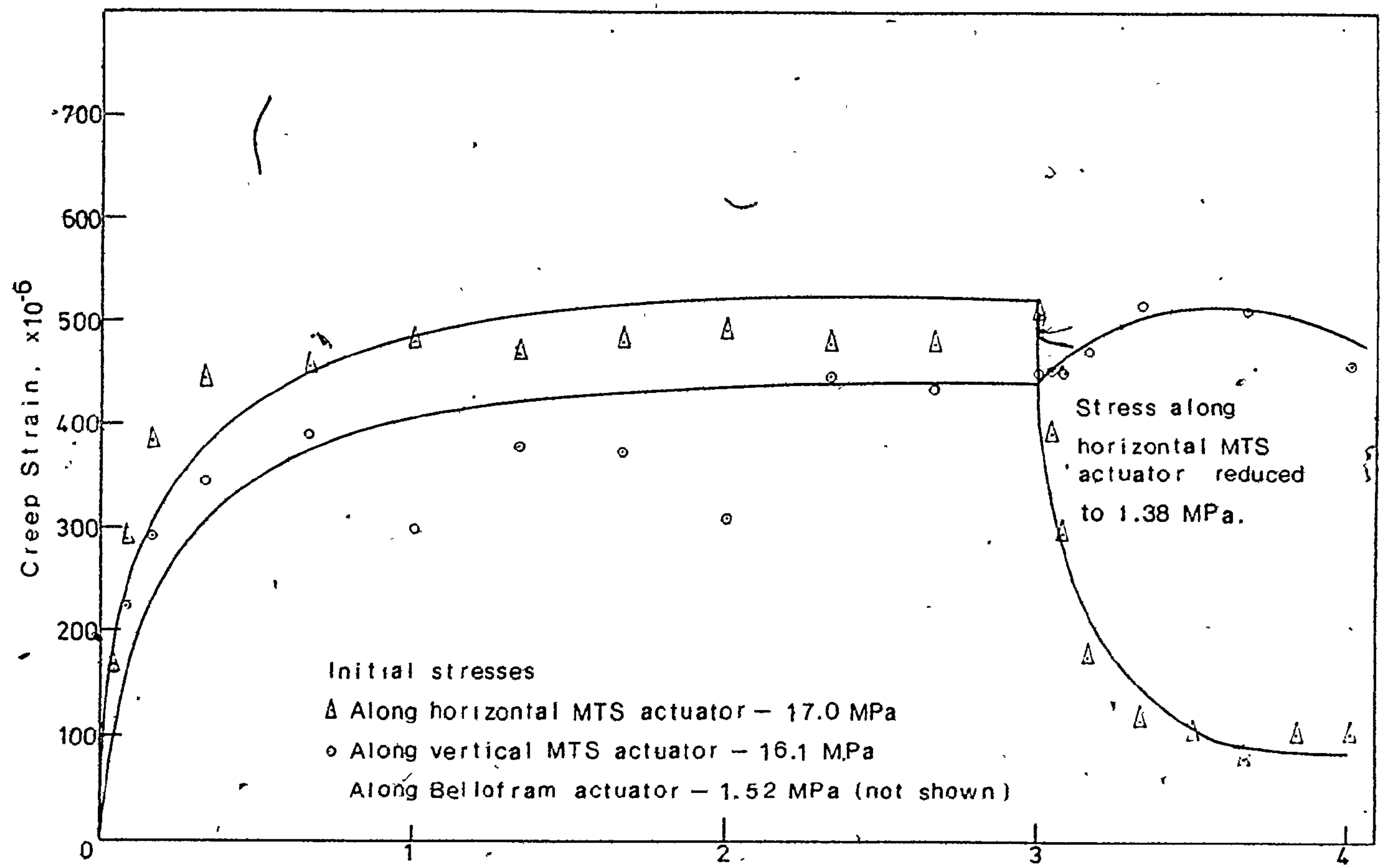

FIGURE A-6 CREEP CURVES: TEST NO.7 – 160 DAYS CURING.